Archives Italiennes de Biologie, 149: 383-405, 2011.

Modulatory effects of the GABAergic basal ganglia neurons on the PPN and the muscle tone inhibitory system in cats

K. TAKAKUSAKI[1], K. OBARA[1], T. NOZU[2], T. OKUMURA[2]

[1] Research Center for Brain Function and Medical Engineering, Asahikawa Medical University, School of Medicine, Midorigaoka-Higashi, Japan;

[2] Department of General Medicine, Asahikawa Medical University, School of Medicine, Midorigaoka-Higashi, Japan

ABSTRACT

Pedunculopontine tegmental nucleus (PPN) contributes to the control of muscle tone by modulating the activities of pontomedullary reticulospinal systems during wakefulness and rapid eye movement (REM) sleep. The PPN receives GABAergic projection from the substantia nigra pars reticulata (SNr), an output nucleus of the basal ganglia. Here we examined how GABAergic SNr-PPN projection controls the activity of the pontomedullary reticulospinal tract that constitutes muscle tone inhibitory system. Intracellular recording was made from 121 motoneurons in the lumbosacral segments in decerebrate cats (n = 14). Short train pulses of stimuli (3 pulses with 5 ms intervals, 10-40 μA) applied to the PPN, where cholinergic neurons were densely distributed, evoked eye movements toward the opposite side and bilaterally suppressed extensor muscle activity. The identical PPN stimulation induced IPSPs, which had a peak latency of 40-50 ms with a duration of 40-50 ms, in extensor and flexor motoneurons. The late-latency IPSPs were mediated by chloride ions. Microinjection of atropine sulfate (20 mM, 0.25 μl) into the pontine reticular formation (PRF) reduced the amplitude of the IPSPs. Although conditioning stimuli applied to the SNr (40-60 μA and 100 Hz) alone did not induce any postsynaptic effects in motoneurons, they reduced the amplitude of the PPN-induced IPSPs. Subsequent injection of bicuculline (5 mM, 0.25 μl) into the PPN blocked the SNr effects. Microinjections of NMDA (5 mM, 0.25 μl) and muscimol (5 mM, 0.25 μl) into the SNr reduced and increased the amplitude of the PPN-induced IPSPs, respectively. These results suggest that GABAergic basal ganglia output controls postural muscle tone by modulating the activity of cholinergic PPN neurons which activate the muscle tone inhibitory system. The SNr-PPN projection may contribute to not only control of muscle tone during movements in wakefulness but also modulation of muscular atonia of REM sleep. Dysfunction of the SNr-PPN projection may therefore be involved in sleep disturbances in basal ganglia disorders.

Key words

Pedunculopontine tegmental nucleus • α-motoneurons • Postsynaptic inhibition • Decerebrate preparation • Muscular tonus • REM sleep

Introduction

Postural muscle tone, which is defined as tonic muscular tension that permit standing, is completely abolished during rapid eye movement (REM) sleep. Sleep disturbances such as insomnias, reduction of REM sleep and REM sleep behavior disorders (RBD) are highly associated with Parkinson's disease (Schenck, 1996; Rye et al., 1997; Ferini-Strambi and Zucconi, 2000; Askenasy, 2001; Larsen

Corresponding Author: Kaoru Takakusaki, MD., Ph.D, Director and Professor, Research Center for Brain Function and Medical Engineering, Asahikawa Medical University, School of Medicine - Tel.: 81-166-68-2884 - Fax: 81-166-68-2887 - Email: kusaki@asahikawa-med.ac.jp

and Tandberg, 2001; Iranzo, 2006; Postuma et al., 2010). Recent clinical studies have suggested the involvement of the neurodegeneration of the mesopontine tegmentum, including the pedunculopontine tegmental nucleus (PPN), in the pathogenesis of RBD (Gagnon et al., 2006; Jubault et al., 2009; Unger et al., 2010).

The PPN has been known as a critical element in the generation and maintenance of the rapid rhythms in the cortex that are associated with wakefulness and REM sleep (Garcial-Rill et al., 1991; Jones 1991; Rye 1997; Datta, 2002; Datta and Siwek, 2002). This nucleus is composed of cholinergic neurons (Armstrong et al., 1983; Rye et al., 1987; Spann and Grofova, 1992; Takakusaki et al., 1996, 1997a, 1997b) and non-cholinergic neurons, including glutamatergic, GABAergic (Ottersen and Storm-Mathisen, 1984; Kosaka et al., 1998; Mena-Segovia et al., 2008) and peptidergic (e.g., Substance P; Vincent et al., 1983) neurons. The PPN has descending projections to the pontomedullary reticular formation in addition to dense ascending projections to the basal ganglia and non-specific thalamic nuclei (Saper and Loewy, 1982; Edley and Graybiel, 1983; Jackson and Crossman, 1983; Mitani et al., 1988; Jones, 1991; Semba and Fibiger, 1992; Lai et. al., 1993; Takakusaki et al., 1996). The PPN receives serotonergic (Muhlethaler et al., 1990; Luebke et al., 1992; Koyama and Kayama, 1993; Fay and Kubin, 2001), noradrenergic (Muhlethaler et al., 1990; Williams and Reiner, 1993) and orexinergic (Peyron et al., 1998; Nambu et al., 1999) projections. The PPN also receives GABAergic projection from the basal ganglia output nuclei, such as the substantia nigra pars reticulata (SNr) and entopeduncular nucleus, which correspond to the internal segment of globus pallidus of primates, in rats (Beckstead et al., 1979; Rye et al., 1987; Spann and Grofova, 1991, 1992) and cats (Moriizumi et al., 1988).

It has been shown that activation of $GABA_B$ receptors on the PPN neurons suppresses generation of REM sleep (Sakai and Koyama, 1996; Ulloor et al., 2004; Datta, 2007). Because GABAergic output from the basal ganglia is thought to be overactive in Parkinson's disease (Delong 1990; Wichmann and Delong, 1996; Takakusaki et al., 2004c; Takakusaki, 2008), it is critical to examine how basal ganglia output to the PPN regulates REM sleep to better understand the mechanisms of reduction of REM sleep and RBD in this disease. Concerning the brainstem-spinal cord mechanisms controlling postural muscle tone, an activation of PPN cholinergic neurons elicited REMs and muscular atonia (Takakusaki et al., 2003a, 2004a, 2004b, 2005). In addition, activation of cholinoceptive pontine reticular formation (PRF) neurons excited medullary reticulospinal tract that exerted postsynaptic inhibitory effects upon hindlimb motoneurons via spinal inhibitory interneurons in decerebrate cats (Takakusaki et al., 1993a, 1994, 2001, 2003b). The above finding lead to the following two hypotheses: 1) the cholinergic PPN neurons activate pontomedullary reticulospinal system that mediates muscular atonia during REM sleep, and 2) GABAergic projection from the SNr to the PPN is responsible for the modulation of motor phenomena of REM sleep (REMs and atonia).

The purpose of the present study was to test the above hypotheses. For this, intracellular recording was made from lumbosacral motoneurons in decerebrate cats. We first identified inhibitory postsynaptic potentials (IPSPs) in hindlimb motoneurons evoked by stimulating the PPN and elucidated whether the characteristics of the IPSPs were equivalent to those induced by stimulation of the pontomedullary reticular formation during naturally-occurring REM sleep (Fung et al., 1982; Chase et al., 1986; Soja et al., 1987). Next we examined whether the PPN-induced IPSPs were evoked by the successive activations of cholinoceptive PRF neurons and medullary reticulospinal neurons. Finally, attempt was made to determine whether GABAergic projections from the SNr to the PPN modulated the PPN-induced IPSPs in motoneurons.

Experimental procedures

All the procedures of the present experiments were approved by the Animal Studies Committee of Asahikawa Medical College in accordance with the Guide for the Care and Use of Laboratory Animals (NIH Guide), revised in 1996. Every attempt was made to minimize animal suffering and to reduce the number of animals used. The study is based on the data from 14 adult cats (raised in an animal laboratory of Asahikawa Medical College) of either sex which weighed from 2.6 to 3.4 kg. The experimental arrangement is schematically illustrated in Fig. 1.

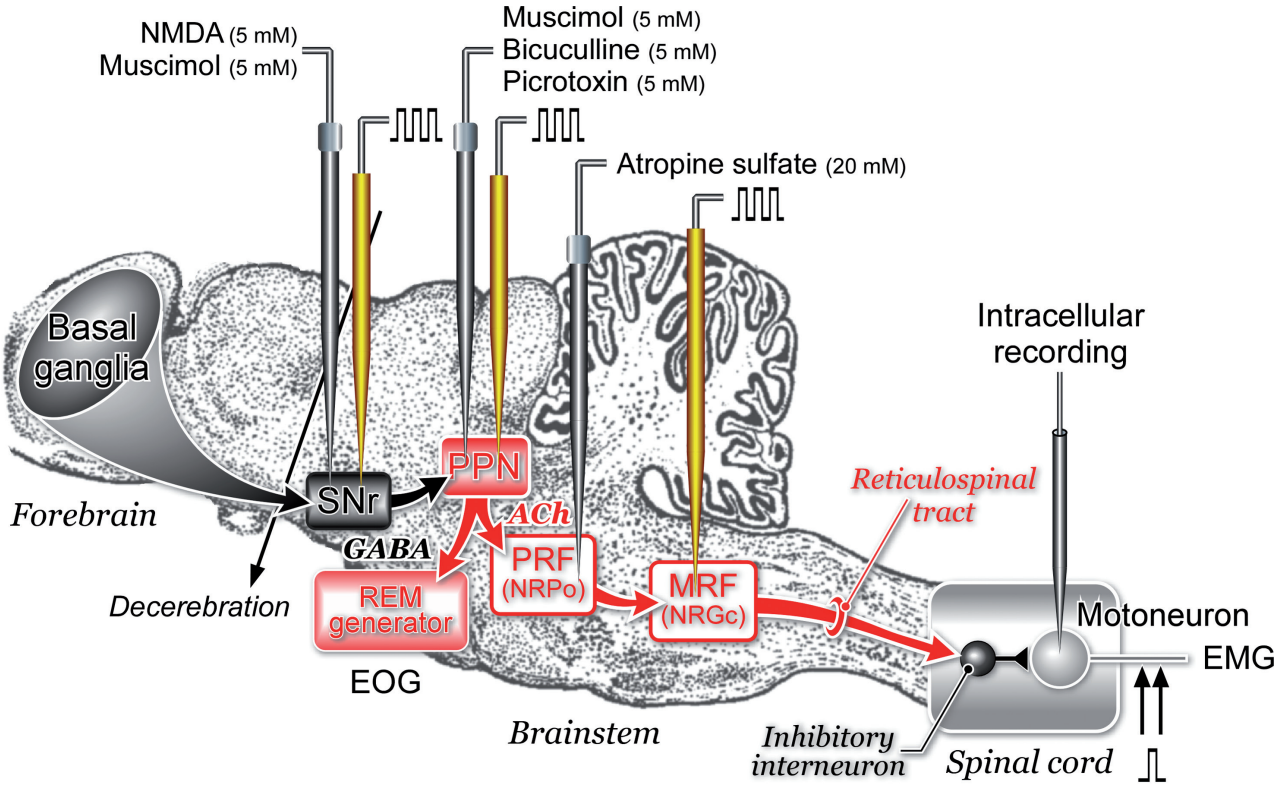

Fig. 1. - Schema of the experimental arrangements used in this study. Abbreviations: Ach = acetylcholine; EMG = electromyograms; EOG = electrooculograms; GABA = gamma-amino-butyric acid; MRF = medullary reticular formation; NRGc = nucleus reticularis gigantocellularis; NRPo = nucleus reticularis pontis oralis; NMDA = N-methyl-D-aspartic acid; PPN = pedunculopontine tegmental nucleus; PRF = pontine reticular formation; REM = rapid eye movement; SNr = substantia nigra pars reticulata. See text for explanations.

Surgical procedures

The trachea of each cat was intubated after the animal was anesthetized with halothane (Flothane, Takeda Co., Osaka, Japan) (0.5-3.0%) and nitrous oxide gas (0.5-1.0 l/min) with oxygen (3.0-5.0 l/min). A cannula was placed in the femoral artery to monitor the blood pressure and in the cephalic vein for administration of pancronium bromide (Myoblock, Sankyo Co., Tokyo, Japan) (0.1 mg/kg). A laminectomy was performed to expose the lumbosacral segments (L4-S1). The animals were surgically decerebrated at the precollicular-postmammillary level. Particular attention was given to avoid injury to the cranial motor nerves for ocular movements, such as the oculomotor, trochlear and abducens nerves. After the surgery, anesthesia was discontinued. The head and the vertebrae of the lumbar segments of each animal were fixed in a stereotaxic apparatus. The rigid spinal frame securely held an animal by pins in the iliac crests, clamps on the dorsal processes of L1-3, and a clamp on the vertebral body of L7. Retraction of the skin permitted the formation of a wall for a pool of oil which covered the exposed cervical and/or lumbosacral cord.

After the surgery, the cat was allowed to assume a reflex standing posture which was due to the decerebrate rigidity. Repetitive stimuli were then delivered to the mesopontine tegmentum so that the optimal stimulation site for producing a collapse of the decerebrate rigidity and eye movements could be determined (Takakusaki et al., 2003a, 2004a).

The cats were again anesthetized with halothane and nitrous oxide gas with oxygen for further surgery to mount peripheral nerves on stimulating electrodes. Two AgCl wires, 0.3 mm diameter and separated by a distance of 2 mm, were used as electrodes for the stimulation of the left hindlimb nerves. The names and abbreviations of the left hindlimb nerves which were dissected and mounted on bipolar electrodes are as follows: quadriceps femoris (Q), tensor fasciae

latae (TFL), posterior biceps-semitendinosus (PBSt), anterior biceps-semimembranosus (ABSm), lateral gastrocnemius-soleus (LG-S), medial gastrocnemius (MG), tibialis anterior (TA), extesorum digitorum longus (EDL), flexorum digitorum longus (FDL), and plantaris (Pl). Throughout an experiment the temperature of the animal's rectum and the oil pool was monitored and maintained at 36-37°C using radiant heat lamps. The end tidal CO_2 was maintained between 4 and 6%. The cats were immobilized by an infusion of pancronium bromide (0.1 mg/kg; Myoblock, Organon, i.v.) and were artificially ventilated during the intracellular recording. The mean blood pressure was maintained at more than 100 mmHg by an i.v. infusion of epinephrine (0.005 ± 0.01 mg/kg; Bosmin, Daiichi Co.) when necessary.

Recording of EMG, EOG and hindlimb motoneurons

Enamel-coated, stainless steel wires (0.5 mm diameter, MT-Giken Co. LTD, Tokyo, Japan) were used to record electromyograms (EMG). Coating of the wires was peeled off over 1 mm length, and a pair of wires was inserted into the bilateral soleus muscles with 2 mm apart to record the EMG. EMG activities were processed with a low pass filter of 5 Hz and a high pass filter of 100 Hz with a time constant of 0.03 s. A pair of stainless screws with a diameter of 0.8 mm was implanted into the lateral part of the anterior wall of the bilateral frontal sinus. They were used to record electrooculograms (EOG). The same style of screw was also implanted into the mid part of the frontal bone as an indifferent electrode. The EOG activity was recorded with a low pass filter of 0.5 Hz and a high pass filter of 200 Hz with a time constant of 0.03 s. Changes in EMG activities of the left and right soleus muscles and those of EOG evoked from each site were rectified, integrated and averaged for 16 sweeps using a signal processor (Model 7T07A, Sanei Co., Tokyo, Japan) (Fig. 2).
Intracellular recordings were obtained from hindlimb motoneurons located at the L6-S1 segments. A glass micropipette filled with 2 M K-citrate or 3 M KCl (tip diameter 1.0-1.5 μm, impedance 5-10 MΩ) was used as a recording electrode. The electrode was connected to a high input impedance preamplifier with negative capacitance compensation (Neurodata model IR 184, Cygnus Technology, Pennsylvania, USA). A reference electrode, which was made from Ag-Cl plate (20 mm length, 5 mm wide and 1 mm thickness) was placed between the cranium and the temporal muscles. Alpha-motoneurons were identified by antidromic invasion from peripheral muscle nerves. They were analyzed only if their antidromic action potentials and membrane potentials exceeded 60 mV (mean 66.3 ± 3.4 mV, n = 121) and -50 mV (mean -60.4 ± 3.6 mV, n = 121), respectively. The membrane potential of each motoneuron was monitored with a low gain DC display. The mean membrane potential was measured by drawing an isopotential line through a polygraph tracing so that it bisected the synaptic noise (Glenn and Dement, 1981a; Takakusaki et al., 1993a). In active cells, a threshold membrane potential for generating action potentials was used as the membrane potential. Anodal current pulses of 50-100 ms duration with an intensity of 0.5-2 nA were also injected intracellularly to estimate the input resistance in the absence of anomalous rectification (Glenn and Dement, 1981b; Takakusaki et al., 1993a; Habaguchi et al., 2002) (Fig. 8). The input resistance was calculated from the voltage shift in response to the current pulses. A glass micropipette filled with 3 M KCl was used to record intracellular activity of motoneuron and to inject chloride ions into the motoneuron so that we could examine whether the PPN-induced inhibitory effects were mediated by chloride ions (Fig. 5C).
A signal processor (Model 7T07A, Sanei Co., Tokyo, Japan) was used to average postsynaptic potentials (PSPs; 8-16 sweeps) evoked by stimulating the PPN and other brainstem areas so that the parameters of the shape of the PSPs could be accurately measured (Fig. 3). Cord dorsum potentials (CDPs) were recorded by means of a platinum ball electrode (1-1.2 mm diameter and 10-20 Ω resistance) placed on the dorsal root entry zone of the rostral L7 segment against a reference electrode inserted into the back muscles. These recordings were used for monitoring the incoming volley from the peripheral nerves. All the records were displayed on a storage oscilloscope and stored for later analysis on magnetic tape (FM recorder, Model LX 10, TEAC Instr., Kanagawa, Japan; bandwidth 0-10.0 kHz).

Brainstem stimulation

A glass micropipette filled with Wood's metal, and with the tip made of a carbon fiber (diameter 6-7 μm, resistance 0.2-0.5 MΩ; Takakusaki et al.,

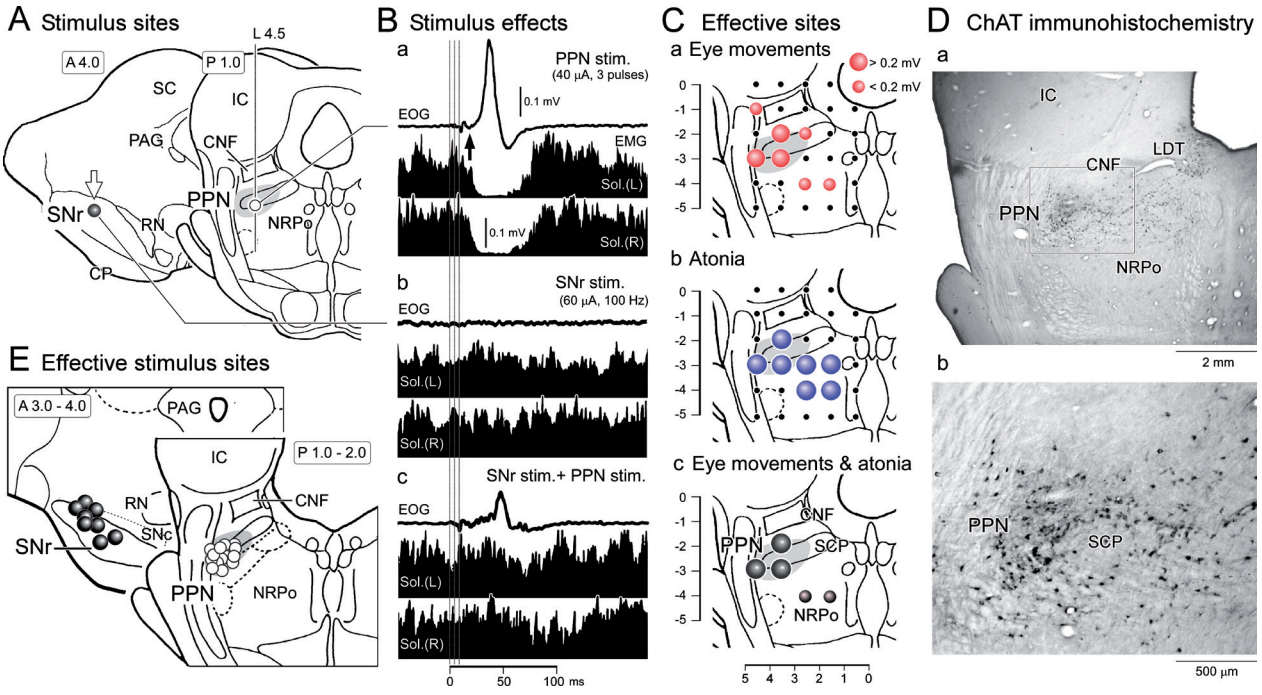

Fig. 2. - PPN-induced muscle tone suppression and eye movement, and their suppression by SNr stimulation. A. Stimulation sites in the PPN and SNr shown on coronal planes of the midbrain (A 4.0) and mesopontine junction (P 1.0). B. (a) Effects of electrical stimulation of the PPN (40 μA, 3 pulses) upon EOG and bilateral soleus EMGs. (b) Conditioning electrical stimulation applied to the SNr (60 μA, 100 Hz) did not evoke any effects in EOG and soleus EMGs. (c) Conditioning SNr stimulation reduced the PPN-induced eye movement and muscle tone suppression. C. Location of effective stimulation sites for evoking eye movements (a), muscular atonia (b) and both (c). The sites where stimulation evoked eye movements larger than 0.2 mV are indicated by large circles in (a). D. Distribution of cholinergic neurons stained by ChAT immunohistochemistry. Light-microscopic photographs with lower and higher magnification are shown in the upper (a) and lower (b) columns, respectively. Abbreviations: CNF = cuneiform nucleus; CP = cerebral peduncle; IC = inferior colliculus; LDT = laterodorsal tegmental nucleus; PAG = periaqueductal grey; RN = red nucleus; SC = superior colliculus; SNc = substantia nigra pars compacta; SCP = superior cerebellar peduncle.

2003a, 2004b) was stereotaxically inserted into the mesopontine tegmentum including the PPN, according to the Horsley-Clark coordinates (anterior (A) 2.0 - posterior (P) 3.0; left or right (LR) 2.0-6.0; horizontal (H) +2.0--5.0; Fig. 1). Short trains of electrical stimuli (3 stimuli with 5 ms intervals and 10-60 μA, 0.2 ms pulse duration) were applied to the mesopontine tegmentum so that optimal site for evoking muscle atonia, eye movements (Fig. 2) and inhibitory postsynaptic potentials (IPSPs) in motoneurons (Figs. 4 and 5) could be identified. For this the stimuli were delivered at 0.5-1.0 mm intervals in the dorsoventral, mediolateral, and rostrocaudal directions. In 8 cats, an identical type of electrode was also inserted into the caudal diencephalon (A 2.0 - A 5.0, LR 3.0-7.0, H +2.0--5.0; Fig. 1). The SNr was stimulated with pulse trains (10-60 μA, 0.2 ms pulse duration, 10-200 Hz). Duration of the stimulation was 10-20 s. The stimuli were delivered at 0.5-1.0 mm intervals in the dorsoventral, mediolateral, and rostrocaudal, directions so that the optimal stimulus sites for inhibiting the PPN-induced effects could be identified (Fig. 8). In 3 cats, stimulating electrode was also inserted into the medullary reticular formation (MRF; Fig. 1) (P 8.0-10.0, L 1.0-2.0, H -4.0--8.0). To examine the MRF stimulus effects on muscle tone, repetitive stimuli (20-50 μA, 0.2 ms duration and a frequency of 50 Hz) were delivered for 5 to 10 seconds. The same stimulating electrode was used to examine effects of MRF stimulation upon motoneurons. Stimulus trains (3 pulses, 5 ms intervals, 10-40 μA), were delivered to the MRF with a frequency of 1 Hz to evoke PSPs (Fig. 6C).

Microinjections of neuroactive substances

A micropipette filled with a solution of one of the following neuroactive substances was inserted into the mesopontine tegmentum (P 1.0-3.0, LR 3.5-4.5, H -1.0--3.5, Fig. 1): muscimol (5.0 mM), a γ-amino butyric acid $(GABA)_A$ receptor agonist or alternatively bicuculline (5.0 mM) or picrotoxin (5.0 mM), $GABA_A$ receptor antagonists. A micropipette of the same type but filled with muscimol (5.0 mM) or N-methyl-D-aspartic acid (NMDA; 5.0 mM), a glutamatergic agonist, was inserted into the SNr area (A 3.0 - A 5.0, LR 3.0-6.0, H -2.0--4.0; Fig. 1). In addition, a micropipette filled with atropine sulfate (20 mM), muscarinic receptor antagonist, was inserted into the cholinoceptive area of the pontine reticular formation (PRF; P 2.0-3.0, LR 1.5-2.5, H -3.0--4.0; Fig. 1). Concentrations were determined on the basis of the findings obtained in previous studies (Takakusaki et al., 2003a, 2004a, 2005). Each substance was injected into the PPN, SNr or PRF areas by using an oil-driven microinjection system (Takakusaki et al., 1993b, 2003a, 2004a, 2005). The volume of each injection was 0.1-0.25 μl and the injection rate was 0.01-0.02 μl/s. All of the substances were dissolved in Ringer solution with pH adjusted to 7.4. Several injections were performed in each animal and an interval of more than 2 hours was allowed between two successive injections.

Changes in the amplitude of PSPs evoked by PPN stimulation were compared before and after injections of these substances into each target area. For statistical analyses, Mann-Whitney U-tests (non-parametric statistics) were employed. Probabilities less than 0.05 were considered as significant. The variability of the means is expressed by the standard deviation (SD) throughout this report.

Histological verification and ChAT immunohistochemistry

At the end of each experiment, the stimulation sites and injection sites of neuroactive substances were marked with electrolytic microlesions which were produced by passing a DC current of 30 μA for 30 s through the stimulating electrode. Animals were then sacrificed by an overdose of pentobarbital anesthesia (Nembutal, 100 mg/kg, i.v., Dainippon Sumitomo Pharma. Co), and the brainstem was removed and fixed in 10% formalin in saline. Later, frozen 50 μm frontal sections or parasagittal sections were cut and stained with cresyl violet. The locations of the microlesions were identified with reference to the stereotaxic atlases of Berman (1968) and Snider and Niemer (1961).

Four of the animals were deeply anaesthetized with Nembutal and transcardially perfused with 0.9% saline followed by a solution of 3.0% paraformaldehyde and 0.01% glutaraldehyde in 0.1 M phosphate buffer (pH 7.4). The brain of each animal was then removed, saturated with a cold solution of 30% sucrose, and 50 μm frozen sections were prepared. Choline acetyltransferase (ChAT) immunohistochemistry was then performed using the peroxidase-antiperoxidase method combined with diaminobenzidine (Mitani et al., 1988; Lai et al., 1993). Monoclonal anti-ChAT antibody (Boehringer Mannheim) was used for these procedures.

Results

Behavioral identification

First, we identified optimal stimulation that evoked muscular atonia in each decerebrate cat. Representative effects obtained from a single cat are shown in Fig. 2A-C. Electrical stimulation consisting of 3 pulses, 5 ms interval and intensity of 40 μA was delivered to the lateral part of the mesopontine tegmentum (Fig. 2A; P 1.0, L 4.5, H-3.0) and evoked eye movements toward the opposite side and bilaterally suppressed soleus muscle activity (Fig. 2Ba). The latency of the onset of eye movement (indicated by an upward arrow) and latency to peak was approximately 15 ms and 30 ms, respectively. The peak amplitude was 0.38 mV. The latency and duration of the suppression of soleus EMG were approximately 20 ms and 60 ms, respectively. Stimulation sites from which eye movements and muscular atonia were evoked in this animal are shown in Fig. 2Ca and 2Cb, respectively. Eye movements with amplitudes larger than 0.2 mV were evoked by stimuli applied to the PPN area, while small eye movements were also evoked by stimuli applied to the PRF corresponding to the nucleus reticularis pontis oralis (NRPo). Atonia-evoking region was also located in the NRPo in addition to the PPN area. Consequently, effective stimulus sites that evoked both eye movements and muscular atonia were mainly located in the PPN area

(Fig. 2Cc). Fig. 2Da shows microphotographic presentation of cholinergic neurons which were labeled at the same antero-posterior level in a different cat by choline-acetyltransferase immunohistochemistry. Higher magnification microphotograph shows that cholinergic neurons are most numerous in the area dorsolateral to the superior cerebellar peduncle (SCP) and are also diffusely distributed in other areas surrounding the SCP (Fig. 2Db). The effective sites for evoking eye movement and muscular atonia well correspond to the area containing a high density of cholinergic neurons.

Repetitive stimulation with 100 Hz and 60 μA was applied to the lateral part of the SNr, which is indicated by an open downward arrow in Fig. 2A. The SNr stimulation itself did not change the level of muscle tone or evoke eye movements (Fig. 2Bb). However, the SNr stimulation combined with PPN stimulation greatly attenuated the PPN-induced eye movement and muscle tone suppression (Fig. 2Bc). The aplitude of eye movement was reduced to 0.1 mV, and peak latency was increased to 50 ms. Fig. 2E shows the locations of stimulation sites on coronal planes of the brainstem in this study. Effective PPN stimulus sites (n = 14) were mainly located in the ventrolateral part of the PPN, and optimal sites where SNr stimulation attenuated the PPN-effects (n = 8) were located in the dorsolateral part of the SNr.

Postsynaptic potentials evoked by stimulating the mesopontine tegmentum

After behavioral identification of the stimulus sites as above, cats were immobilized and intracellular recording was made from hindlimb motoneurons. Short trains of stimuli (3 pulses, 40 μA, 5 ms interval) were applied to the mesopontine tegmentum, including the PPN. Examples in Fig. 3A are PSPs evoked by stimulating the muscle tone inhibitory region in the

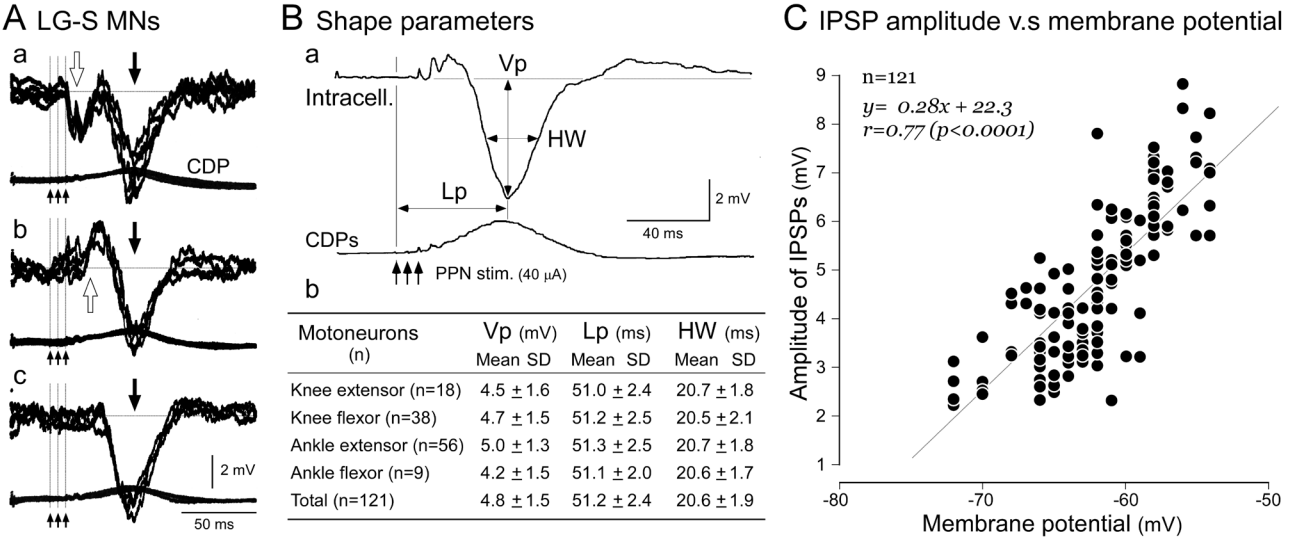

Motoneurons (n)	Vp (mV) Mean	SD	Lp (ms) Mean	SD	HW (ms) Mean	SD
Knee extensor (n=18)	4.5	±1.6	51.0	±2.4	20.7	±1.8
Knee flexor (n=38)	4.7	±1.5	51.2	±2.5	20.5	±2.1
Ankle extensor (n=56)	5.0	±1.3	51.3	±2.5	20.7	±1.8
Ankle flexor (n=9)	4.2	±1.5	51.1	±2.0	20.6	±1.7
Total (n=121)	4.8	±1.5	51.2	±2.4	20.6	±1.9

Fig. 3. - Characteristics of postsynaptic potentials evoked by PPN stimulation. A. Postsynaptic potentials observed in three LG-S motoneurons in one cat. In each set of recordings, the upper and lower traces are intracellular potentials and cord dorsum potentials (CDP), respectively. There is a mixture of excitatory and inhibitory postsynaptic potentials with early (~20 ms) and late (30-70 ms) latencies. IPSPs with late latency (filled arrows) were observed in all three motoneurons. Early latency IPSPs and EPSPs were evoked in motoneurons (a) and (b), respectively. Only a late-latency IPSP was evoked in motoneuron (c). B. (a) Shape indices of the PPN-induced IPSPs: peak voltage (Vp), latency to peak (Lp) and half-width (HW). Example of the PPN-induced IPSPs in a PBSt motoneuron was averaged over 16 sweeps. (b) Means and standard deviations (SD) of the shape parameter of the IPSPs observed in four groups of motoneurons. Knee extensors (18 motoneurons) include Q (n = 12) and TFL motoneurons (n = 6). Knee flexors (38 motoneurons) include PBSt (n = 22) and ABSm (n = 16) motoneurons. Ankle extensors (56 motoneurons) include LG-S (n = 31), MG (n = 10), FDL (n = 9) and plantaris (n = 6) motoneurons. Ankle flexors (9 motoneurons) include TA (n = 5) and EDL (n = 4) motoneurons. In (A) and (B), pulses of PPN stimuli are denoted by upward arrows below the CDP. C. Changes in the amplitude of the PPN-induced IPSPs as a function of the prestimulus membrane potential level. There was a positive correlation between these parameters. An equilibrium potential which was calculated from the regression line was estimated at -79.6 mV.

PPN in 3 LG-S motoneurons in a single cat. There is a mixture of excitatory (EPSPs) and IPSPs with early (~20 ms) and late (30-70 ms) latencies. In motoneuron (a), IPSPs with early (open arrow) and late (filled arrow) latencies were observed. Motoneuron (b) received excitation with a short latency (upward arrow) and inhibition with a longer latency. Only late latency IPSPs were observed in motoneuron (c). The late IPSPs (downward arrows) were invariably observed in all motoneurons (n = 121), while there were variations in early latency PSPs.

Shape parameters of the late IPSPs are shown in Fig. 3Ba. Three parameters were measured: peak voltage (Vp), latency to peak (Lp) and half-width (HW). Peak voltage or amplitude of the IPSPs was 4.8 ± 1.5 mV (mean ± SD), Lp was 51.2 ± 2.4 ms, and HW was 20.6 ± 1.9 ms. These parameters of the late IPSPs are shown in each motoneuron group innervating knee extensor (n = 18), knee flexor (n = 38), ankle extensor (n = 56), and ankle flexor (n = 9) muscles. There was no difference in these parameters among the different groups of motoneurons (Fig. 3Bb). On the other hand, amplitude of the IPSPs was positively correlated with the prestimulus membrane potential ($p < 0.0001$). The equilibrium potential of the IPSPs which was calculated from the regression line was estimated at approximately -80 mV (-79.6 mV).

In Fig. 4A, optimal stimulation sites for evoking the late IPSPs were examined by moving stimulating electrode tip in rostro-caudal and dorso-ventral directions on parasagittal plane of the brainstem. IPSPs with the maximum amplitude were evoked by stimuli applied to the site of H -3.0 and P 1.0 (indicated by an arrow). The amplitude of late IPSPs was reduced if stimuli were applied to rostral, caudal, dorsal or ventral sites. The optimal sites for evoking the late IPSPs were located in the area corresponding to the PPN. Similarly, dorsoventral and mediolateral distributions of effective sites were examined on the contralateral (right) coronal plane of the mesopontine tegmentum (Fig. 4B). Large amplitude IPSPs were evoked by stimulating the sites at R 5.0 and H -3.0 (indicated by an arrow) which also corresponded to the PPN. The amplitudes of the IPSPs were reduced when stimuli were applied to surrounding sites. On the other hand, stimulation applied to the NRPo, which was medial to the PPN, also induced IPSPs.

Fig. 5A shows effects of stimulating the mesopontine tegmentum in 5 different (Q, PBSt, ABSm, LG-S and FDL) motoneurons in a single cat. In each motoneuron, late IPSPs with the maximum amplitude were evoked by stimuli applied to the same site in the PPN (indicated by arrow). Amplitude of the IPSPs in each motoneuron was reduced when stimuli were applied to the sites dorsal or ventral to the optimal location. Injection of hyperpolarizing current gradually reduced the amplitude of the late IPSPs, and their polarity was finally reversed (Fig. 5B). Similarly, an injection of chloride ion also reversed the polarity of the late IPSPs (Fig. 5C). These findings suggest that the PPN-induced late IPSPs were induced by inward current mediated by chloride ions.

PPN-induced late IPSPs are mediated by cholinergic projections to the PRF

Next, examination was made whether cholinergic neurons in the PPN were involved in the generation of PPN-induced IPSPs. Stimulation was applied to the PPN area (downward arrow in Fig. 6Aa) and atropine sulfate was microinjected into the PRF (arrow head in Fig. 6Aa). PPN stimulation evoked early EPSPs followed by late IPSPs (Fig. 6Ab). Following pontine atropine injection, amplitude of the late IPSPs was reduced and that of the early EPSP was increased (Fig. 6Ac). The difference between these potentials, which is shown in Fig. 6Ad, demonstrated that pontine atropine injection removed both early and late inhibitory effects. The effects of pontine atropine injection were studied in 10 motoneurons. Changes in the amplitude of EPSPs and IPSPs are summarized in Fig. 6B. There was a trend for increased amplitude of the early EPSP but the difference was not statistically significant. However, the amplitude of the late IPSPs was significantly reduced following pontine atropine injections from 4.8 ± 1.8 mV to 2.5 ± 0.7 mV (mean ± SD).

We then tested whether the PPN-induced IPSPs were mediated by activation of the medullary reticulospinal tract. Stimulation of the PPN (indicated by a filled arrow in Fig. 6Ca) with 10 μA did not evoke inhibitory effects upon LG-S motoneuron (Fig. 6Cb). Stimulation applied to the medullary reticular formation, which corresponded to the nucleus reticularis gigantocellularis (NRGc; an open arrow in Fig. 6Ca), with 10 μA evoked late IPSP (Fig. 6Cc).

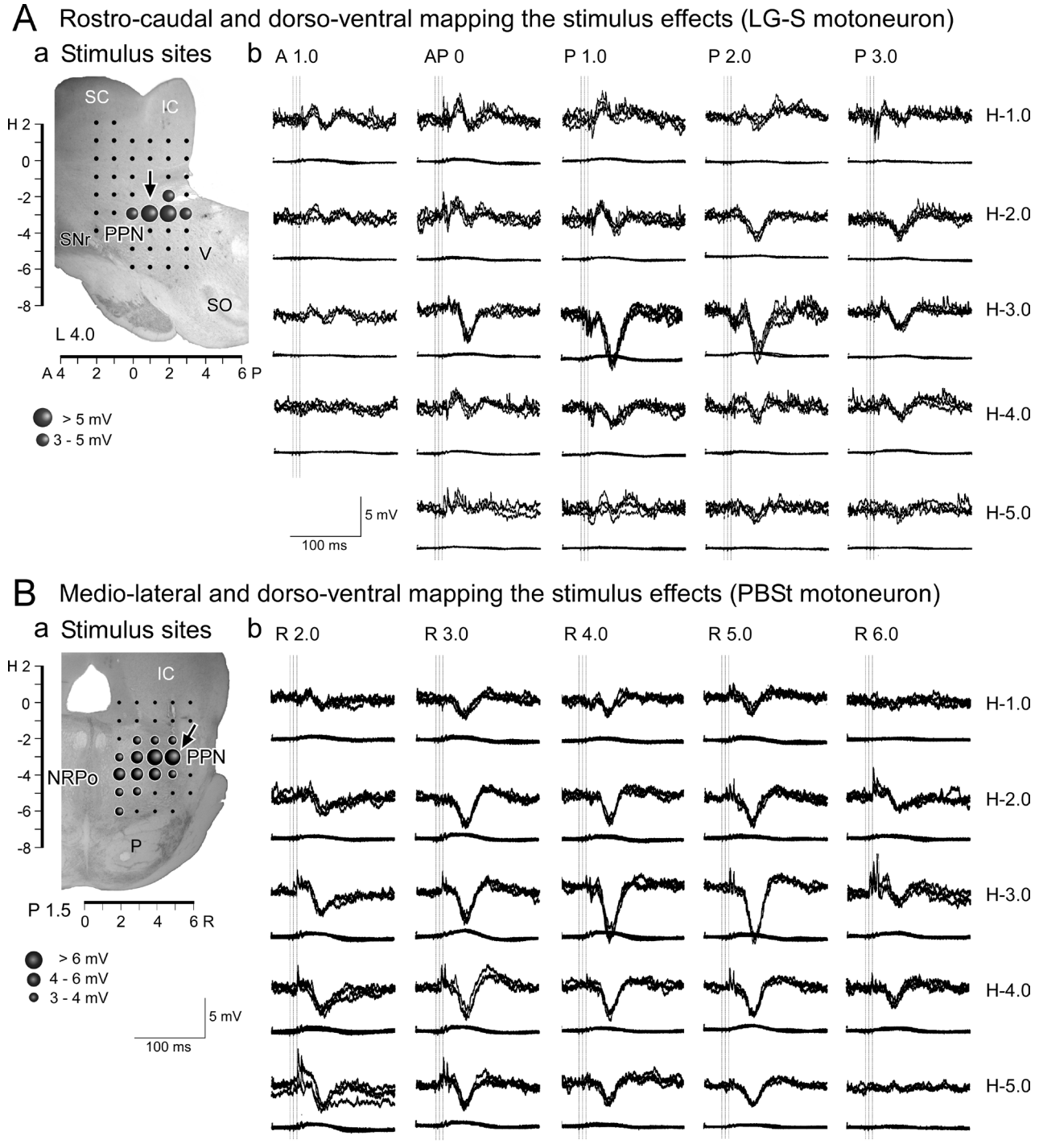

Fig. 4. - The optimal mesopontine tegmental stimulation sites for evoking the late inhibitory effects in hindlimb motoneurons. A. (a) The effective stimulation sites for evoking late IPSPs in an LG-S motoneuron in a parasagittal plane of L 4.0. (b) Postsynaptic potentials evoked by stimulation at A 1.0, AP 0, P 1.0, P 2.0 and L 3.0 at depths of H -1.0, H -2.0, H -3.0, H -4.0 and H -5.0 in the parasagittal plane shown in (a). B. (a) Effective stimulation sites for evoking late IPSPs in a PBSt motoneuron in a coronal plane of P 1.5. (b) Postsynaptic potentials evoked by stimulation at R 2.0, R 3.0, R 4.0, R 5.0 and R 6.0, and at depths of H -1.0, H -2.0, H -3.0, H -4.0 and H -5.0 in the coronal plane of (a). In each record, the upper and lower traces are intracellular potentials and CDP, respectively. The size of a filled circle indicates the amplitude of the IPSPs. Large circles denote stimuli that produced large IPSPs in the motoneurons. In (A) and (B), arrows indicate the sites where stimulation evoked IPSPs with the largest amplitude in each motoneuron. Pulses of stimuli are denoted by vertical dashed lines. Abbreviations: V = trigeminal nucleus; P = pyramis; SO = superior olive.

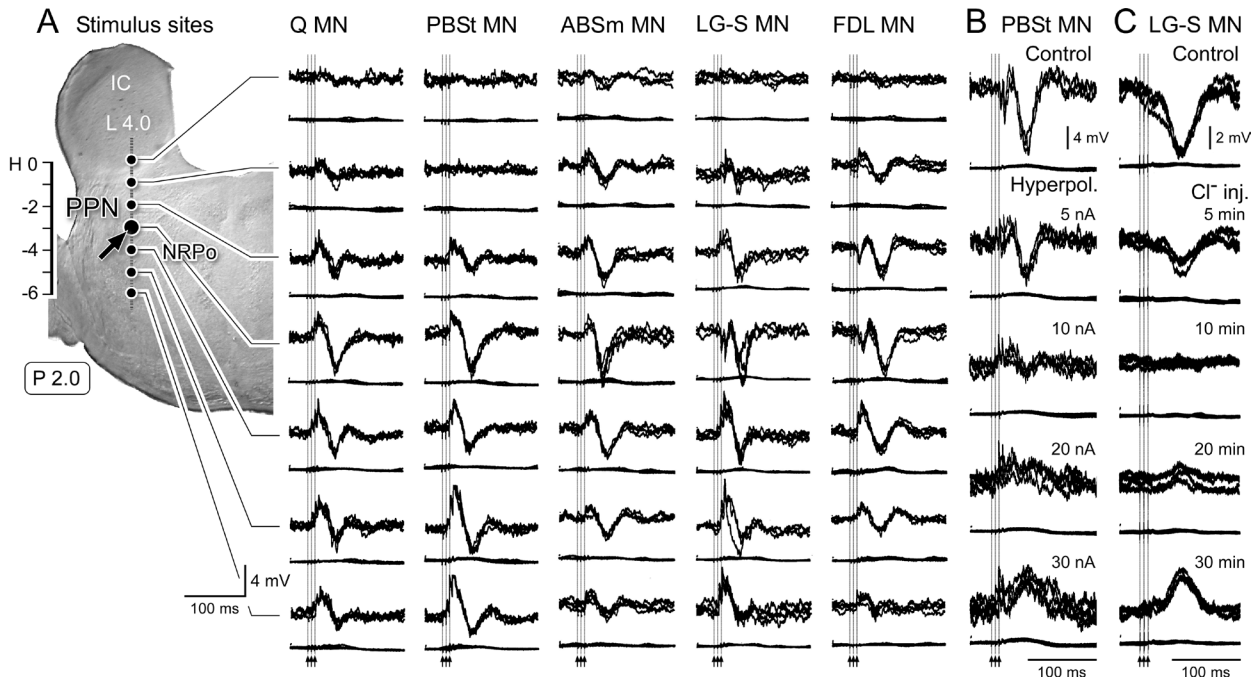

Fig. 5. - Postsynaptic potentials in hindlimb motoneurons evoked by stimulation in the lateral part of the mesopontine tegmentum. A. Mesopontine stimulation sites shown on a coronal plane at P 2.0 and L 4.0. Postsynaptic effects of stimulation at each site in motoneurons innervating Q, PBSt, ABSm, LG-S and FDL muscles. The arrow in A indicates the site where stimulation evoked the largest amplitude IPSP in all motoneurons. Stimulation consisted of 40 μA, 3 pulses with 5 ms intervals. B. Reversal of IPSPs in a PBSt motoneuron by intracellular injection of hyperpolarizing (Hyperpol.) current (current intensity is shown in the upper right former of each panel). C. Reversal of IPSPs in a LG-S motoneuron by intracellular injection of chloride (Cl^-) ions. The total duration of injection is shown in upper right corner of each panel. In each set of recordings, the upper and lower traces are intracellular potentials and CDP, respectively. The arrows beneath the CDP indicate the stimulus pulses.

The conditioning subthreshold PPN stimulation increased the amplitude of the NRGc-induced IPSP from 2 mV (Fig. 6Cc) to 6 mV (Fig. 6Cd). However such a facilitatory effect was attenuated by atropine injection (Fig. 6Ce) into the NRPo (indicated by an arrowhead in Fig. 6Ca). Accordingly, the PPN inhibitory effects can be mediated by cholinoceptive PRF neurons and the medullary reticulospinal neurons.

GABAergic modulation of the PPN-induced inhibitory effects upon motoneurons

Attempts were further made to investigate how injections of GABA receptor agonist and antagonist modulated the effects of PPN stimulation. Representative findings are shown in Fig. 7. Stimulation of the PPN (indicated by a downward arrow in Fig. 7A) induced late IPSPs which were preceded by early excitatory effects in a PBSt motoneuron (Fig. 7Ab). Then muscimol, $GABA_A$-receptor agonist, was injected into the PPN area adjacent to the stimulation site (indicated by an arrowhead in Fig. 7Aa). Muscimol injection did not change the amplitude of the excitatory effects but greatly reduced the amplitude of the IPSPs (Fig. 7Ac). Difference of these PSPs clearly demonstrated that the PPN muscimol injection only removed the late inhibitory effects (Fig. 7Ad). Effects of muscimol injections into the PPN were studied in 12 motoneurons. The reduction of the amplitude of the late IPSPs by muscimol injections was statistically significant (Fig. 7Ca).

Next, $GABA_A$-receptor antagonists, such as picrotoxin or bicuculline, were injected into the PPN so that GABAergic effects upon PPN neurons could be removed (Fig. 7B). In a PBSt motoneuron, PPN stimulation induced early EPSP and late IPSP (Fig. 7Ba). Picrotoxin injection into the PPN area which was adjacent to the stimulation site remarkably increased the amplitude of the late IPSP (Fig. 7Bb) in addition to reducing the amplitude of the early

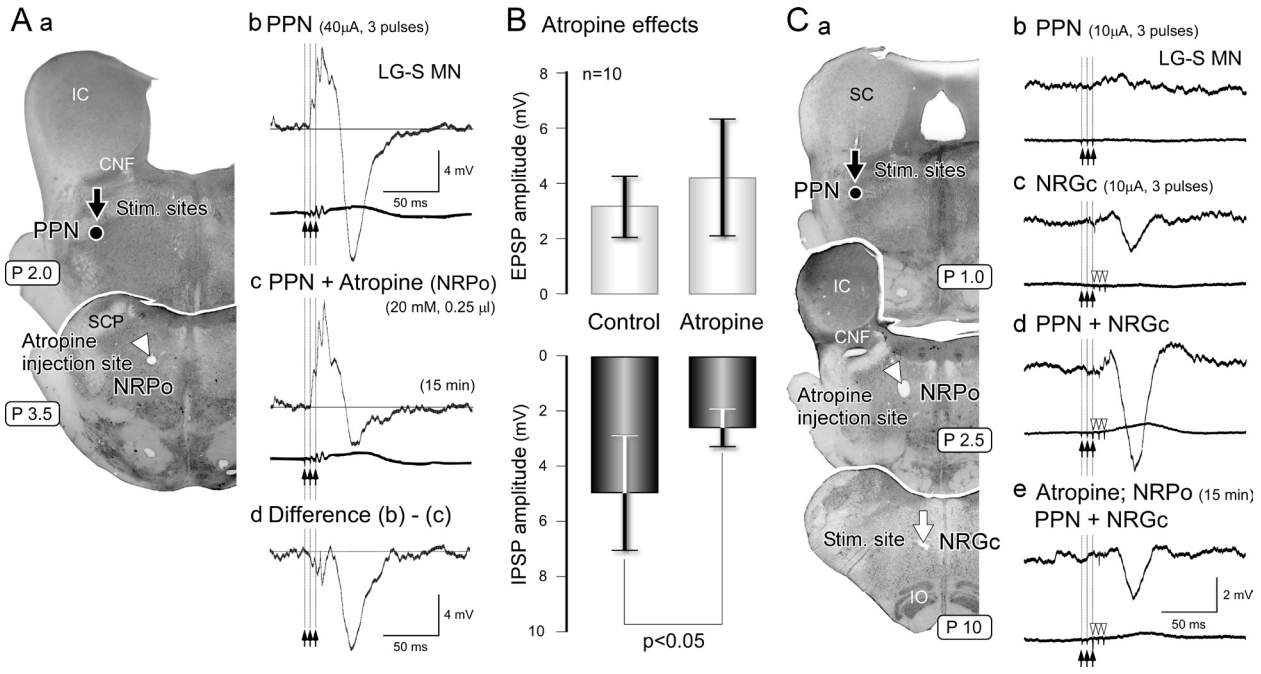

Fig. 6. - Effects of pontine atropine injections on PPN-induced IPSPs. A. (a) Stimulation site in the PPN (arrow) and atropine injection site in the NRPo (arrow-head) shown on coronal planes of the mesopontine tegmentum at P 2.0 and P 3.0, respectively. (b) PPN-induced PSPs in an LG-S motoneuron. (c) Changes in the PSPs measured 15 min after pontine atropine injection. (d) Difference between these two potentials. B. Changes in the amplitude of PPN-induced PSPs following atropine sulfate injections into the NRPo were examined in 10 motoneurons. The amplitudes of control EPSPs and IPSPs were 3.1 ± 1.1 mV and 4.9 ± 2.1 mV, respectively. After atropine injections, the amplitudes of the EPSPs and IPSPs were 4.2 ± 2.1 mV, and 2.6 ± 0.8 mV, respectively ($p < 0.05$). C. (a) Locations of stimulation site in the PPN (filled arrow), atropine injection site in the NRPo (arrowhead), and stimulation site in the NRGc (open arrow) shown on coronal planes of the pons and medulla. (b) Effect of conditioning PPN stimulation (upward arrows below the CDP), which was subthreshold to evoke IPSPs (10 μA and 3 pulses with 5 ms intervals) in an LG-S motoneuron. (c) Late-latency IPSPs evoked by stimulation in the NRGc (10 μA and 3 pulses with 5 ms intervals). The stimuli are denoted by open arrowheads above the CDP. Conditioning stimulation of the PPN increased the amplitude of the NRGc-induced IPSPs. (d) Fifteen minutes after atropine injection into the NRPo, the facilitatory effects were greatly attenuated. Each recording was averaged over 16 sweeps.

EPSP. The difference between these potentials (Fig. 7Bc) clearly demonstrated that picrotoxin injection facilitated inhibitory effects. Effects of picrotoxin and bicuculline were examined in 3 and 4 motoneurons, respectively. Injection of these $GABA_A$-receptor antagonists into the PPN significantly increased the size of the late IPSPs (Fig. 7Cb) but did not alter the amplitude of the EPSPs. These findings suggest that excitability of PPN neurons that are responsible for the inhibitory effects is modulated by $GABA_A$ receptors in the PPN region.

Basal ganglia modulation of the PPN-inhibitory effects upon motoneurons

The last part of our investigations was to evaluate how GABAergic input from the SNr to the PPN modulated PPN-effects upon motoneurons (Figs. 8-10). Stimulation of the PPN (indicated by a downward arrow in Fig. 8Ab) evoked IPSPs with early and late latencies in a PBSt motoneuron (Fig. 8Ae). Conditioning stimuli, which consisted of 100 Hz and 60 μA, were then applied to the lateral part of the midbrain including the SNr in a dorsoventral direction along an axis of A 3.5 and L 5.5 with 1 mm intervals (Fig. 8Af) so that these stimuli could modulate inhibitory effects from the PPN. When the conditioning stimuli were applied to the SNr (H -3), amplitude of the PPN-induced IPSPs was greatly reduced. However, the reduction was not prominent when conditioning stimuli were applied to the dorsal (H -1) or ventral (H -5) sites. Although the SNr stimulation reduced the amplitude of the PPN-induced IPSPs, it did not reduce the input

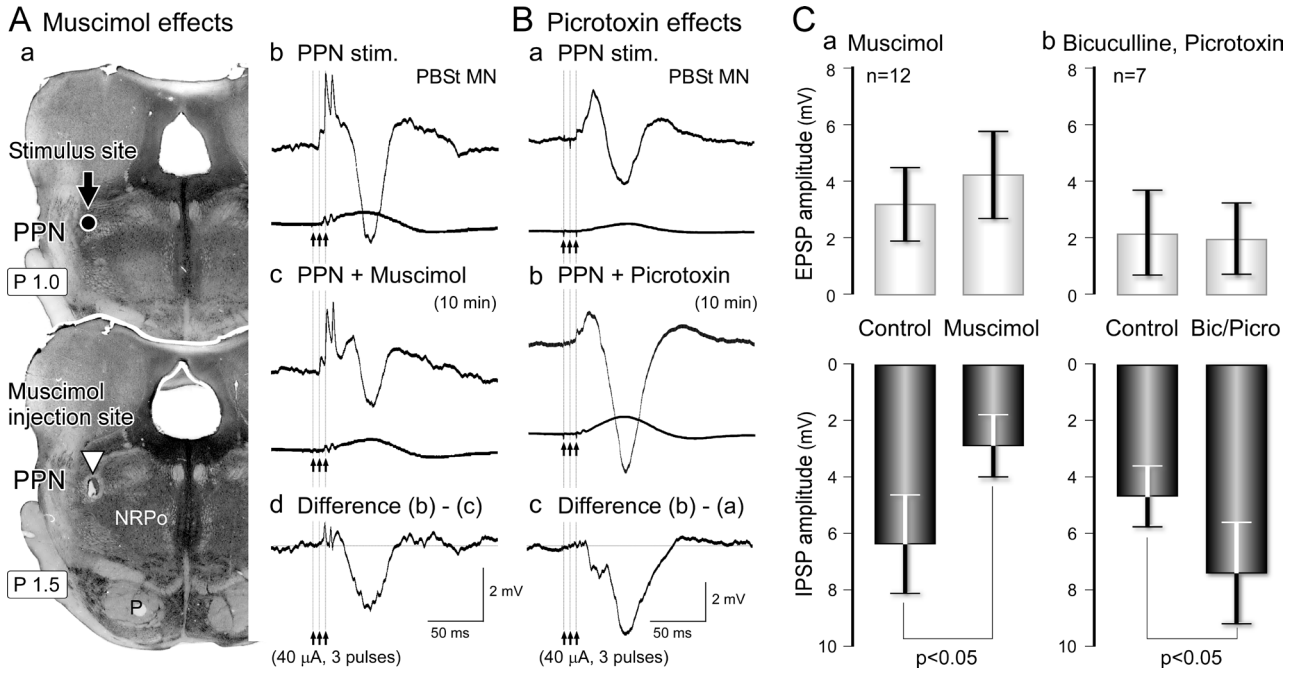

Fig. 7. - Effects of injections of GABAergic agents into the PPN on PPN-evoked potentials in lumbar motoneurons. A. Effects of muscimol injection into the PPN. (a) Stimulation site in the PPN (arrow) and muscimol injection site in the NRPo (arrowhead) shown on coronal planes of the mesopontine tegmentum at P 1.0 and P 1.5, respectively. (b) PPN-induced PSPs in a PBSt motoneuron. (c) Changes in the PSPs 10 min after PPN muscimol injection. (d) Difference between these two potentials. B. Effects of picrotoxin injection into the PPN. (a) PPN-induced PSPs in a PBSt motoneuron. (b) Changes in the PSPs at 10 minutes after PPN picrotoxin injection. (c) Difference in these two potentials. C. (a) Changes in the amplitude of PPN-induced PSPs in 12 motoneurons after muscimol injections into the PPN. The amplitudes of the control EPSPs and IPSPs were 3.2 ± 1.3 mV and 6.4 ± 1.7 mV, respectively. After injections, amplitude of the EPSPs and IPSPs were 4.3 ± 1.5 mV, and 2.9 ± 1.1 mV, respectively. Changes in IPSPs were statistically significant ($p < 0.05$). (b) Changes in the amplitude of PPN-induced PSPs in 7 motoneurons after injections of bicuculline or picrotoxin into the PPN. Amplitude of control EPSPs and IPSPs were 2.1 ± 1.6 mV (mean ± SD) and 4.7 ± 1.1 mV, respectively. After injections, the amplitudes of the EPSPs and IPSPs were 1.9 ± 1.3 mV, and 7.4 ± 1.7 mV, respectively ($p < 0.05$). Each recording was averaged over 16 sweeps.

resistance of the same motoneuron (Fig. 8Ac and Ad). Examination was also made in an LG-S motoneuron of the same animal (Fig. 8Ba). Conditioning stimuli were applied along the axis of A 3.5 and L 4.5 with 1 mm intervals (Fig. 8Aa). It was observed that the amplitude of both the early and late IPSPs was reduced by the conditioning stimuli applied to the SNr at H-3 and H-4 (Fig. 8Bb).

In a different animal, stimulation was applied at intervals of 1.0 mm to the lateral part of the mesopontine tegmentum along an axis of P 2.0 and L 4.0 (Fig. 8Ca). In an LG-S motoneuron, combinations of EPSPs and IPSPs were evoked by stimuli applied at each site. The late IPSP was evoked from the PPN (3rd trace in Fig. 8Cc), which is indicated by a filled arrow in Fig. 8Cb. Conditioning stimulation of the SNr (open circle in Fig. 8Ca) nearly eliminated the late IPSPs (3rd and 4th traces in Fig. 8Cd) while the EPSPs were not affected (1st, 2nd, 5th and 6th traces in Fig. 8Cd) or even facilitated (3rd and 4th traces in Fig. 8Cd).

The effects of SNr stimulation depended on the stimulus frequency (Fig. 9). Stimulation of the PPN (filled arrow in Fig. 9Ab) induced late IPSP (Fig. 9Ba). Conditioning stimuli were applied to the SNr (open arrow in Fig. 9Aa) with various frequencies from 25 to 200 Hz (Fig. 9Bb). The size of the PPN-IPSPs was reduced by the SNr stimuli with each frequency; the reduction was maximal when SNr was stimulated with a frequency of 100 Hz. The reduction of the IPSPs was less prominent if stimulus frequency was either higher or lower than 100 Hz. Substantial findings were obtained from another 4 motoneurons. It was consistent that the most prominent suppressive effect was evoked by SNr stimuli at a frequency of 100 Hz. Moreover, the

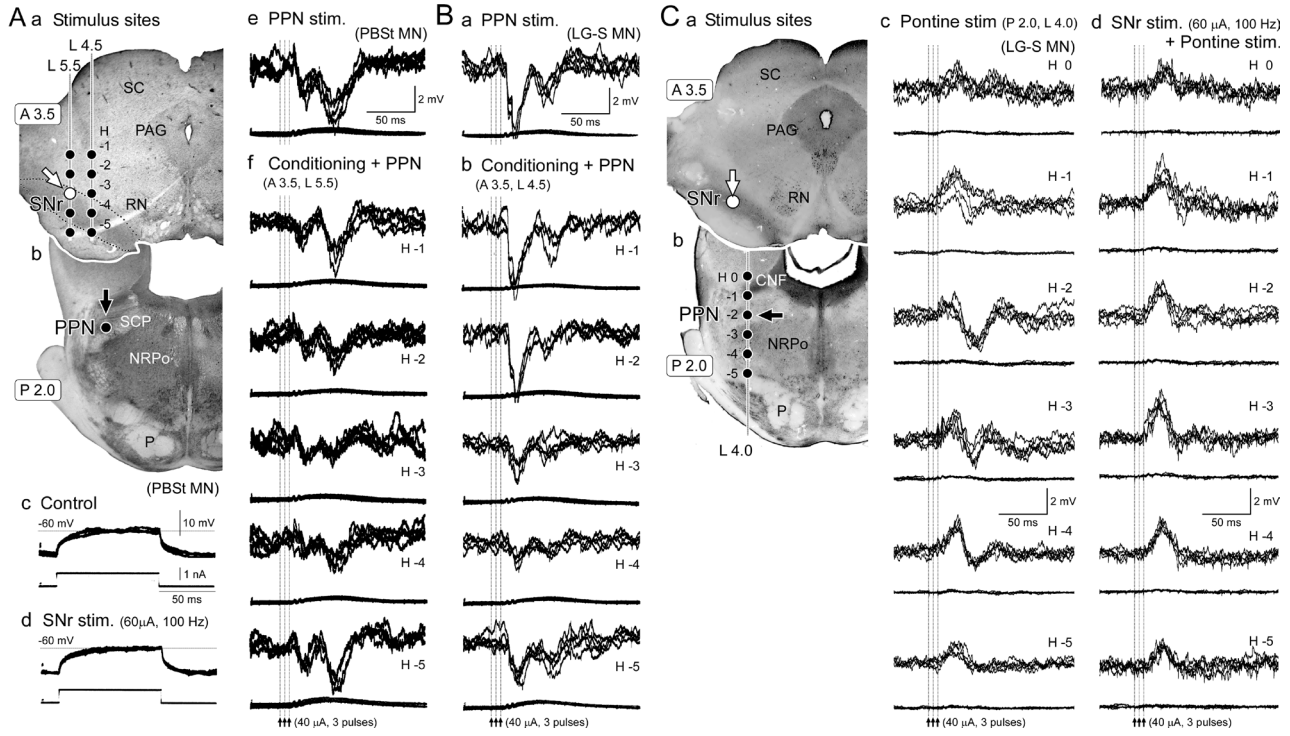

Fig. 8. - Effects of stimulation within the SNr on PPN-induced IPSPs in lumber motoneurons. A. (a) Stimulation sites in the midbrain including the SNr, shown on coronal plane at A 3.5. Conditioning stimulation consisted of 60 μA with 100 Hz. Stimuli were applied at L 4.5 and L 5.5. Open arrow indicates the optimal stimulation site from which inhibitory action on PPN-IPSPs was most prominent. (b) Stimulation site in the PPN. (c)-(d) Membrane potential shifts in response to the depolarizing pulse in a PBSt motoneuron before (c) and during (d) SNr stimulation. SNr stimulation did not alter input resistance. (e) Early and late IPSPs evoked by PPN stimulation. (f) Changes in the PPN-induced IPSPs following conditioning stimulation applied to sites from H -1.0 to H -5.0 at A 3.5 and L 5.5, as shown in (Aa). B. (a) Early and late IPSPs evoked by PPN stimulation. (b) Changes in the PPN-induced IPSPs following conditioning stimulation applied to sites from H -1.0 to H -5.0 along an axis of A 3.5 and L 4.5, which is shown in (Aa). Note that the IPSPs were maximally reduced when conditioning stimuli were applied to the SNr (H-4.0). (A) and (B) were obtained from the same animal. C. (a) A site of conditioning stimulation in the SNr shown on coronal plane at A 3.5 (open arrow). (b) Stimulation sites in the lateral part of the mesopontine tegmentum including the PPN, at P 2.0 and L 4.0. Filled arrow indicates the stimulation site which corresponds to the PPN. (c) Postsynaptic potentials in an LG-S motoneuron evoked by stimuli applied to sites shown in (b). (d) Effects of conditioning stimulation of the SNr (60 μA with 100 Hz) on the effects of mesopontine stimulations. IPSP components were nearly abolished SNr stimulation.

suppressive action of the SNr stimulation was due to activation of GABAergic projections from the SNr. As shown in Fig. 9D, stimulation of the PPN (Fig. 9Ab) induced late IPSPs preceded by early EPSPs in a PBSt motoneuron (Fig. 9Db). Although conditioning SNr stimulation (Fig. 9Aa) itself did not evoke any potentials in this motoneuron (Fig. 9Da), it reduced the size of the PPN-induced late IPSPs without altering the early EPSPs (Fig. 9Dc). Subsequent bicuculline injection into the PPN (indicated by an arrowhead in Fig. 9Ac) increased the amplitude of the PPN-induced IPSP (Fig. 9Dd). The SNr conditioning stimulation did not reduce the size of the PPN-induced IPSPs (Fig. 9De).

A final examination was conducted to determine whether stimulation of glutamatergic or GABAergic receptors on SNr neurons contributed to alteration of the PPN-effects. For this changes in the PPN-induced IPSPs were studied after injections of NMDA, glutamatergic agonist or muscimol into the SNr (Fig. 10). Stimulation of the PPN (an arrow in Fig. 10Aa) evoked early EPSPs followed by late IPSPs (Fig. 10Ab). After injection of NMDA into the SNr (an arrowhead in Fig. 10Aa), the amplitude of the late IPSP was reduced and that of the early EPSP was increased (Fig. 10Ac). The difference between these postsynaptic potentials indicated that the NMDA injection removed IPSP components

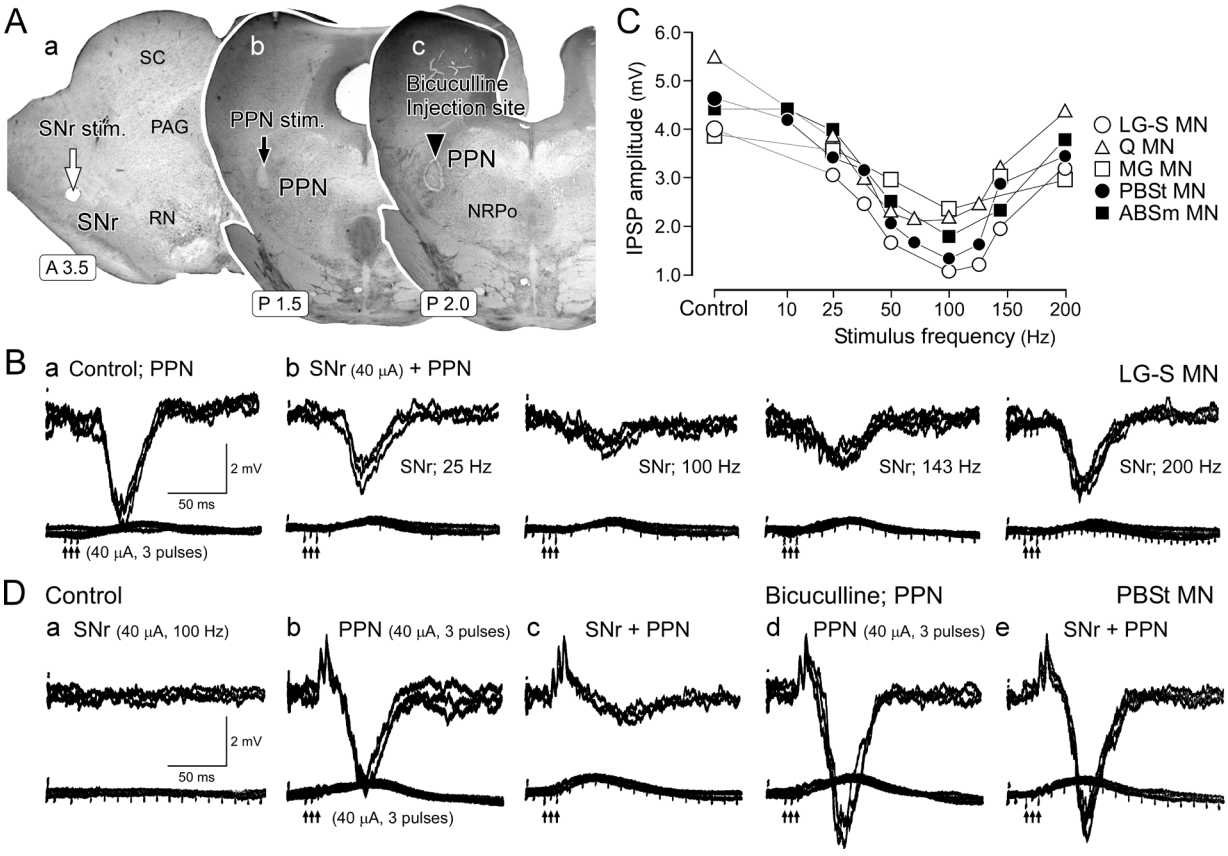

Fig. 9. - Characteristics of the effects of SNr stimulation on PPN-induced IPSPs in lumbar motoneurons. A. (a)-(b) Stimulation sites in the SNr (open arrow) and the PPN (filled arrow) on the coronal planes at A 3.5 and P 1.5, respectively. (c) Bicuculline injection site in the PPN (arrowhead) shown on the coronal plane at P 2.0. B. (a) Postsynaptic potentials evoked by PPN stimulation (40 μA, 3 pulses) in an LG-S motoneuron. (b) Effects of changes in SNr stimulus frequency from 25 to 200 Hz on the PPN-induced IPSPs. Note that conditioning SNr stimulation with a frequency of 100 Hz maximally reduced the PPN-evoked IPSPs. C. Effects of changing the SNr stimulus frequency on PPN-induced IPSPs in five motoneurons. The amplitude of the IPSPs was reduced in relation to the increase in SNr stimulation frequency up to 100 Hz. However, the PPN-evoked IPSPs were less reduced when SNr was stimulated with frequencies higher than 100 Hz. D. Postsynaptic effects evoked by conditioning SNr stimulation (40 μA, 100 Hz) (a), PPN stimulation (40 μA, 3 pulses) (b), and combined SNr and PPN stimulation (c). Conditioning SNr stimulation greatly reduced the amplitude of the PPN-induced IPSPs (c). Bicuculline injection into the SNr increased the amplitude of the PPN-induced IPSPs (d) and it blocked the SNr effects (e).

(Fig. 10Ad). In a different animal, muscimol injection into the SNr increased the amplitude of the PPN-induced late IPSP (Fig. 10Ba and b). The difference between these potentials clearly demonstrated that PPN-effects were enhanced by a reduction of activity in SNr neurons (Fig. 10Bc). The effects of NMDA and muscimol injections into the SNr were examined in 10 and 9 motoneurons, respectively. The amplitude of the PPN-evoked IPSPs was significantly decreased and increased by NMDA and muscimol injections into the SNr, respectively (Fig. 10Ca and Cb).

Discussion

Considerations of the effects evoked by PPN stimulation

The present results confirmed the previous findings that stimulation of the PPN induced muscle tone suppression and REMs (Takakusaki et al., 2004b, 2005), and the muscle tone suppression was due to postsynaptic inhibition of motoneurons (Takakusaki et al., 2004a). Precise mapping the stimulus effects in the mesopontine tegmentum (Figs. 4 and 5) revealed that the optimal stimulation sites for evoking the inhibitory effects corresponded to the caudo-

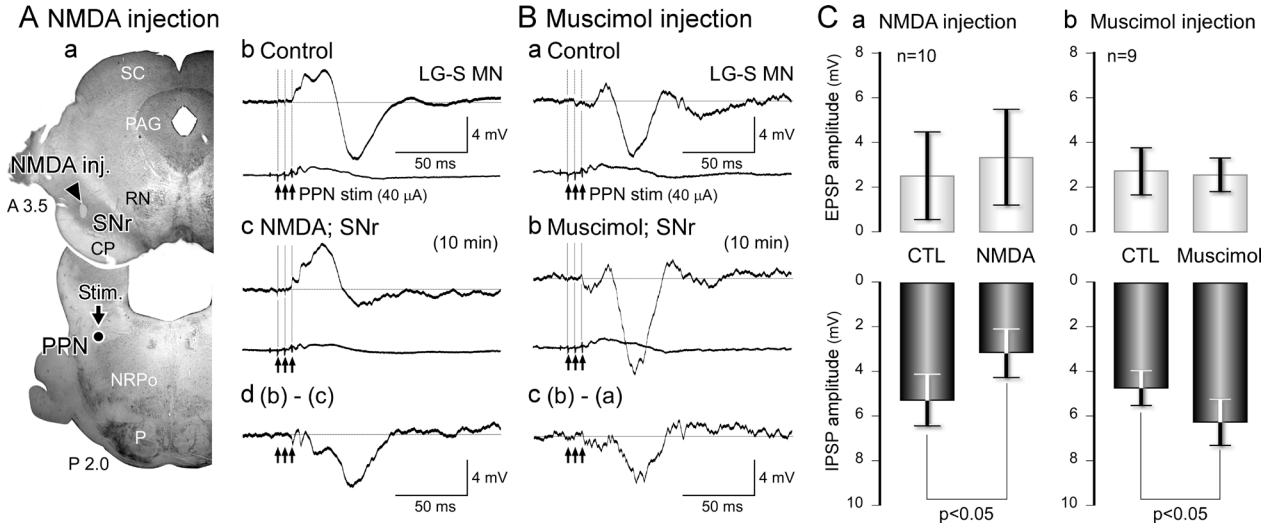

Fig. 10. - Effects of injecting NMDA and muscimol into the SNr on PPN-evoked potentials in lumbar motoneurons. A. Effects of NMDA injection into the PPN. (a) Stimulation site in the PPN (arrow) and NMDA injection site in the SNr (arrow head) shown on coronal planes of the mesopontine tegmentum and the midbrain, respectively. (b) PPN-induced PSPs in an LG-S motoneuron. (c) Changes in the PSPs 10 min after NMDA injection into the SNr. (d) Difference between these two potentials. Each recording was averaged over 16 sweeps. B. Effect of muscimol injection into the SNr. (a) PPN-induced PSPs in an LG-S motoneuron. (b) Changes in the PSPs 10 min after SNr muscimol injection. (c) Difference between these two potentials. Each recording was averaged over 8 sweeps. C. (a) Changes in the amplitude of PPN-induced PSPs in 10 motoneurons after NMDA injections into the SNr. The amplitudes of the control EPSPs and IPSPs were 2.5 ± 2.0 mV and 5.3 ± 1.2 mV, respectively. After injections, the amplitudes of the EPSPs and IPSPs were 3.4 ± 2.1 mV, and 3.2 ± 1.1 mV, respectively ($p < 0.05$). (b) Changes in the amplitude of PPN-induced PSPs in 9 motoneurons after injections of muscimol into the PPN. The amplitudes of the control EPSPs and IPSPs were 2.7 ± 1.1 mV and 4.7 ± 0.7 mV, respectively. After injections, the amplitudes of the EPSPs and IPSPs were 2.5 ± 0.7 mV, and 6.2 ± 1.0 mV, respectively ($p < 0.05$).

ventro-lateral part of PPN where cholinergic neurons were densely distributed. However, electrical stimulation also possibly activated non-cholinergic neurons because the PPN is composed of heterogeneous neuronal populations of neurons; cholinergic, GABAergic, and glutamatergic neurons (Clements and Grant, 1990; Ford et al., 1995; Mena-Segovia et al., 2009) and a variety of other neuronal markers, including calcium-binding proteins and neuropeptides (Fortin and Parent, 1999; Vincent, 2000). In addition, the stimulation also activated passing fibers. Nonetheless, the inhibitory effects of PPN stimulation are considered to be evoked by activation of GABA-responsive cholinergic neurons for the following reasons. First, muscimol and picrotoxin injections into the PPN significantly changed the amplitude of IPSPs without altering the EPSPs (Fig. 7). Second, the IPSPs were further reduced by atropine injections into the PRF (Fig. 6).

In contrast, EPSPs evoked by PPN stimulation were not reduced by pontine atropine injections, indicating that the excitatory effects were not mediated by cholinergic neurons projecting to the PRF. It should be noted that the magnitude of the PPN-induced EPSPs was changed by alteration of the IPSPs. For example, injection of picrotoxin into the PPN (Fig. 7C) and that of NMDA into the SNr (Fig. 10A) tended to increase the amplitude of EPSPs while having the opposite effect on the late IPSPs. Also, electrical stimulation of the SNr attenuated the PPN-induced IPSPs but facilitated EPSPs (Fig. 8C). Possibly, the amplification of the EPSP was due to dis-inhibition. Short trains of stimuli applied to the PPN evoked eye movements in addition to suppression of muscle tone (Fig. 2). What are mechanisms of the PPN-induced eye movements? It has been shown that both REM and PGO waves are prominent phasic events of REM sleep which occur concurrently. PGO-on neurons were recorded in discrete regions of the brachium conjunctivum including the PPN (Datta and Hobson, 1994; Koyama and Sakai, 2000) and in the caudal PRF (Pivik et al., 1977). Vanni-Mercier and Debilly (1998) provided evidence for a parallel organization of the oculomotor and PGO wave

systems, and suggested the existence of interconnections between the mesopontine cholinergic nuclei and the caudoventral PRF that operate as a common generator of REM and PGO waves. Therefore, one explanation for PPN-induced eye movements is that stimulation of the PPN activated the PGO-on neurons, resulting in generation of eye movements via caudoventral PRF neurons. A projection from the superior colliculus (SC) to the paramedian PRF where saccade generator is located contributes to saccadic eye movements (Hikosaka et al., 2000). Moreover, a projection from the PPN to the SC is thought to induce express saccades (Kobayashi et al., 2004). Therefore alternative explanation would be that PPN stimulation activated SC neurons to generate eye movements.

Then, how did SNr stimulation attenuated the PPN-induced eye movements? Datta et al. (1991) demonstrated that a subpopulation of SNr neurons projecting to the PPN area exhibited tonically increased firing preceding the PGO wave, and suggested that an enhancement in SNr neurons' discharges leads to hyperpolarization (inhibition) of PGO-related neurons. Accordingly, it is possible that SNr stimulation inhibited PGO related neurons in the PPN, resulting in suppression of REM generation. Another possibility is that SNr stimulation inhibited SC neurons responsible for saccade generation via a projection to paramedian PRF. During naturally-occurring REM sleep, López-Rodríguez et al. (1990, 1992) demonstrated REM sleep specific IPSPs in conjunction with PGO waves. Because the time-course of the PGO-related IPSPs was mostly the same as that evoked by PPN stimulation, we favor the idea that activation of cholinergic PPN neurons mediates the generation of PGO waves, REM and muscular atonia during REM sleep.

Brainstem and spinal cord mechanisms of muscle tone suppression

Activation of cholinoceptive PRF neurons induced muscular atonia in chronic (Baghdoyan et al., 1984, 1987; Vanni-Mercier et al., 1989; Yamamoto et al., 1990; Kubin, 2001; Márquez-Ruiz and Escudero 2009) and acute decerebrate cats (Morales et al., 1987; Takakusaki et al., 1993a, 1993b, 1994; Fenik et al., 1998). A reticulospinal tract descending from the NRGc is considered to inhibit motoneurons (Chase et al., 1986; Takakusaki et al., 1989, 1994, 2001, Xi et al., 2001a; Habaguchi et al., 2002). In the present study, subthreshold PPN stimulation increased amplitude of the NRGc-induced IPSPs, while it was greatly attenuated by an injection of atropine sulphate into the NRPo (Fig. 6C). These findings corroborated that cholinoceptive PRF neurons contributed to muscle tone suppression via reticulospinal tract arising from the NRGc.

The time course of the late IPSPs evoked from the PPN was mostly the same as that of IPSPs evoked by stimulating the pontomedullary reticular formation (Fung et al., 1982; Chase et al., 1986; Soja et al., 1987; López-Rodríguez et al., 1990; Xi et al., 2001a, 2001b) during naturally-occurring REM sleep in cats. López-Rodríguez et al. (1990) demonstrated that REM sleep-specific IPSPs evoked by NRGc stimulation were mediated by inward chloride ion currents through glycine receptors on motoneurons. As shown in Fig. 3C, the PPN-induced IPSPs were also mediated by inward current of chloride ions. These findings suggest that stimulation of the PPN activate pontomedullary reticulospinal system which mediates inhibition of motoneurons during REM sleep. Moreover, we presume that the motor inhibition can be mediated by lamina VII interneurons in the lower lumber segment, because they were activated by stimulation of the NRGc (Takakusaki et al., 2003b).

It has been shown GABA receptors on PRF neurons are involved in muscle tone control during wakefulness and sleep. Injections of GABA receptor agonist and antagonists into the NRPo prolonged episodes of wakefulness with an increase in motor activity and induced muscular atonia, respectively (Xi et al., 1999, 2001a, 2001b). Similarly, GABA receptors on the PPN neurons are involved in the regulation of REM sleep (Fogel et al., 2010). For example, $GABA_A$ receptors within the PPN facilitate the generation of REM sleep by suppressing the activity of waking-related processes within this nucleus (Torterolo et al., 2001). In contrast Pal and Mallick (2009) showed that injections of $GABA_A$ receptor agonist and antagonist into the PPN increased and reduced the amount of REM sleep, respectively. On the other hand, Ulloor et al. (2004) demonstrated that $GABA_B$ receptors rather than $GABA_A$ receptors on PPN cholinergic neurons are involved in the regulation of REM sleep. The present study clearly demonstrated that microinjections of $GABA_A$-receptor

agonist and antagonists into the PPN reduced and facilitated the PPN-induced motor inhibition (Fig. 7). Because monoaminergic systems such as the coerulospinal (Fung and Barnes, 1981) and raphespinal (Sakai et al., 2000) tracts are considered as muscle-tone facilitatory systems, how are they involved in the PPN-induced muscle tone suppression? Recently, Lai et al. (2010) studied the changes in the release of noradrenaline (NA), serotonin (5-HT), GABA, glycine and glutamate in the spinal cord during motor inhibition induced by electrical stimulation of the MRF including the NRGc in the decerebrate cat. Stimulation of the MRF increased a release of glycine and GABA, and decreased a release of NA and 5-HT in the ventral horn of the lumbosacral cord. However, glutamate levels were not changed by the MRF stimulation. These results together with the present findings suggest that PPN-induced muscle tone suppression can be due to excitation of muscle tone inhibitory system and inhibition of the monoaminergic excitatory systems.

Basal ganglia modulation of the activity of muscle tone inhibitory system

PPN inhibitory effects were suppressed by conditioning stimulation applied to the SNr (Figs. 8 and 9), and the suppressive effect was blocked by injections of $GABA_A$ receptor antagonists into the PPN (Fig. 9). Moreover, injections of NMDA and muscimol into the SNr reduced and facilitated the PPN-inhibitory effects, respectively (Fig. 10). These findings indicate that PPN neurons, which are responsible for muscle tone inhibition, are under the tonic inhibitory control of GABAergic neurons in the SNr (Takakusaki et al., 2003a, 2004b). In addition, GABAergic neurons of the entopeduncular nucleus may contribute to the regulation of PPN activity, because the PPN-effects were suppressed by stimuli applied to the area dorsal to the SNr (Fig. 8A) where entopeduncular GABAergic neurons descended (Moriizumi et al., 1988; Saitoh et al., 2003, 2004). Effects of SNr stimulation were prominent if stimuli were applied with a frequency of 100 Hz (Fig. 9). Because spontaneous firing rate of SNr neurons was approximately between 30-100 Hz in the alert monkey (Hikosaka and Wurtz, 1985), a frequency within this range can be a critical determinant in the control of muscle tone, locomotion, and saccadic eye movements (Hikosaka et al., 2000). However, the SNr effects were attenuated during stimulation with frequencies higher than 150 Hz. This phenomenon leads to an important concept: an intervention which blocks the abnormal activity of the SNr in Parkinsonism by high frequency stimulation could potentially restore the normal function of the brainstem centers that control muscle tone and locomotion (Takakusaki et al., 2003a). Various mechanisms, including depolarization block and stimulation-evoked release of GABA caused by the high-frequency stimulation, have been proposed for the inactivation of neurons in the basal ganglia nuclei (Dostrovsky and Lozano, 2002; Vitek, 2002). Chastan et al. (2009) demonstrated that high frequency stimulation of the SNr (130-190 Hz) dramatically improved axial motor symptoms such as gait failure and postural disturbances in Parkinson's disease patients. Moreover, deep brain stimulation of the PPN with low frequency (~25 Hz) applied to the patients with idiopathic Parkinson's disease not only improved gait failure (Stefani et al., 2007) by altering spinal cord excitability (Pierantozzi et al., 2008) but also significantly improved executive functions and working memory, and beneficially alleviated sleep architecture (Alessandro et al., 2010).

How do basal ganglia contribute to the regulation of sleep?

Sleep disturbance is an early sign of Parkinson's disease (Ferini-Strambi and Zucconi, 2000; Askenasy, 2001; Larsen and Tandberg, 2001). There are several reports suggesting that nearly a half of Parkinson's disease patients who were diagnosed with idiopathic RBD but were free of neurodegenerative diseases had developed Parkinson's disease (Schenck, 1996; Rye et al., 1999; Iranzo, 2006; Boeve, 2007; Postuma et al., 2010). Postuma et al. (2010) concluded that the severity of REM atonia loss in idiopathic RBD predicts Parkinson's disease. A neuronal loss in the PPN was reported in Parkinson's disease (Hirsch et al., 1987), and the loss of cholinergic neurons in the PPN is possibly related to the disability of patients with Parkinson's disease (Rinne et al., 2008).

Several mechanisms are postulated in relation to the basal ganglia regulation of sleep. On the one hand, recent brain imaging studies revealed that a damage in the brainstem, particularly the pontomedullary reticular formation, is critically involved in the pathogenesis of RBD (Jubault et al., 2009; Unger et al., 2010). Jubault et al. (2009) demonstrated

using magnetic resonance imaging (MRI) that brainstem damage may be the first identifiable stage of Parkinson's disease neuropathology, and suggested that the brainstem damage could explain some non-motor symptoms of this disease which often precede diagnosis, such as autonomic dysfunction and sleep disorders. On the other hand, dopaminergic influence of the basal ganglia in the control of sleep-wake behavior also has been suggested (Mena-Segovia et al., 2008). Vetrivelan et al. (2010) postulate that dopaminergic system modulates sleep and wakefulness states via projections to the basal ganglia structures and extra-basal ganglia structures such as the limbic system. It is also possible that basal ganglia efferents to the non-specific thalamic nuclei may affect sleep-awake states by modulating the activity of ascending reticular activating system (ARAS). Since the classical study of Moruzzi and Magoun (1949), the pontomesencephalic reticular formation has been known to comprise the ARAS. The PPN has been considered as a part of the ARAS (Garcia-Rill, 1991; Jones, 1991; Inglis and Winn, 1995; Steriade, 1996). In addition to the PPN, the SNr has a direct projection to the thalamic nuclei (Hendry et al., 1979; Parent et al., 1983; Paré et al., 1990). Because PPN has dense projections to the midbrain dopaminergic neurons, activity of the PPN neurons may affect sleep-awake states by modulating dopaminergic systems projecting to the basal ganglia and extra-basal ganglia areas. Consequently, our idea is that basal ganglia output from the SNr may affect the sleep-awake cycle by modulating the activity of the ARAS through dual systems. One system is through a direct nigro-thalamic projection, and the other, which is considered in this study, by indirect connections via the PPN (Takakusaki et al., 2004c, 2006).

Conclusion

The present study clearly demonstrated that postsynaptic inhibitory effects evoked by the PPN stimulation was due to the activation of cholinergic neurons in the PPN, which subsequently excited cholinoceptive PRF neurons and the medullary reticulospinal neurons (muscle tone inhibitory system). Moreover, injections of NMDA and muscimol into SNr altered PPN-induced IPSPs, indicating that GABAergic projection from the SNr regulated postural muscle tone by modulating the activity of cholinergic PPN neurons. Because the GABAergic basal ganglia output is thought to be overactive in parkinsonian patients (Delong, 1990; Wichmann and Delong, 1996), the present findings can be strongly related to the sleep disturbance in Parkinson's disease associated with SNr dysfunction.

Acknowledgements

This work is supported by Grants-in-Aid for Scientific Research (C) and Priority Areas "Emergence of Adaptive Motor Function through Interaction between Body, Brain and Environment (Area #454)" from the Japanese Ministry of Education, Culture, Sports, Science and Technology to K.T.

References

Alessandro S., Ceravolo R., Brusa L., Pierantozzi M., Costa A., Galati S., Placidi F., Romigi A., Iani C., Marzetti F., Peppe A. Non-motor functions in parkinsonian patients implanted in the pedunculopontine nucleus: focus on sleep and cognitive domains. *J. Neurol. Sci.*, **289**: 44-48, 2010.

Armstrong D.A., Saper C.B., Levey A.I., Winer B.H., Terry R.D. Distribution of cholinergic neurons in the rat brain demonstrated by the immunohistochemical localization of choline acetyltransferase. *J. Comp. Neurol.*, **216**: 53-68, 1983.

Askenasy J.J. Approaching disturbed sleep in late Parkinson's disease: first step toward a proposal for a revised UPDRS. *Parkinsonism Relat. Disord.*, **8**: 123-131, 2001.

Baghdoyan H.A., Rodrigo-Angulo M.L., McCarley R.W., Hobson J.A. Site-specific enhancement and suppression of desynchronized sleep signs following cholinergic stimulation of three brain-stem region. *Brain Res.*, **306**: 39-52, 1984.

Baghdoyan H.A., Rodrigo-Angulo M.L., McCarley R.W., Hobson J.A. A neuroanatomical gradient in the pontine tegmentum for the cholinoceptive induction of desynchronized sleep signs. *Brain Res.*, **414**: 245-261, 1987.

Beckstead R.M., Domesick V.B., Nauta W.J.H. Efferent connections of the substantia nigra and ventral tegmental area in the rat. *Brain Res.*, **175**: 191-217, 1979.

Berman AL. *The brain stem of the cat: cytoarchitectonic atlas with stereotaxic coordinates.* Madison: University of Wisconsin Press, 1968.

Boeve B.F., Silber M.H., Saper C.B., Ferman T.J., Dickson D.W., Parisi J.E., Benarroch E.E., Ahlskog J.E., Smith G.E., Caselli R.C., Tippman-Peikert M., Olson E.J., Lin S.-C., Young T., Wszolek Z., Schenck C.H., Mahowald M.W., Castillo P.R., Del Tredici K., Braak H. Pathophysiology of REM sleep behaviour disorder and relevance to neurodegenerative disease. *Brain*, **130**: 2770-2788, 2007.

Chase M.H., Morales F.R., Boxer P.A., Fung S.J., Soja P.J. Effect of stimulation of the nucleus reticularis gigantocellularis on the membrane potential of cat lumbar motoneurons during sleep and wakefulness. *Brain Res.*, **386**: 237-244, 1986.

Chastan N., Westby G.W., Yelnik J., Bardinet E., Do M.C., Agid Y., Welter M.L. Effects of nigral stimulation on locomotion and postural stability in patients with Parkinson's disease. *Brain*, **132**: 172-184, 2009.

Clements J.R. and Grant S. Glutamate-like immunoreactivity in neurons of the laterodorsal tegmental and pedunculopontine nuclei in the rat. *Neurosci. Lett.*, **120**: 70-73, 1990.

Datta S., Curró Dossi R., Paré D., Oakson G., Steriade M. Substantia nigra reticulata neurons during sleep-waking states: relation with ponto-geniculo-occipital waves. *Brain Res.*, **566**: 344-347, 1991.

Datta S. and Hobson J.A. Neuronal activity in the caudolateral peribrachial pons: relationship to PGO waves and rapid eye movements. *J. Neurophysiol.,* **71**: 95-109, 1994.

Datta S. Evidence that REM sleep is controlled by the activation of brain stem pedunculopontine tegmental kainate receptor. *J. Neurophysiol.*, **87**: 1790-1978, 2002.

Datta S. and Siwek D.F. Single cell activity patterns of pedunculopontine tegmentum neurons across the sleep-wake cycle in the freely moving rats. *J. Neurosci. Res.*, **15**: 611-621, 2002.

Datta S. Activation of pedunculopontine tegmental PKA prevents $GABA_B$ receptor activation-mediated rapid eye movement sleep suppression in the freely moving rat. *J. Neurophysiol.*, **97**: 3841-3850, 2007.

Delong, M.R. Primate models of movement disorders of basal ganglia origin. *Trends Neurosci.*, **13**: 281-289, 1990.

Dostrovsky J.O. and Lozano A.M. Mechanisms of deep brain stimulation. *Mov. Disord.*, **17** Suppl. 3: S63-68, 2002.

Edley S.M. and Graybiel A.M. The afferent and efferent connections of the feline nucleus tegmenti pedunculopontinus, pars compacta. *J. Comp. Neurol.*, **217**:187-215, 1983.

Fay R. and Kubin L. 5-HT_{2A} receptor-like protein is present in small neurons located in rat mesopontine cholinergic nuclei, but absent from cholinergic neurons. *Neurosci. Lett.*, **314**: 77-81, 2001.

Fenik V., Davies R.O., Pack A.I., Kubin L. Differential suppression of upper airway motor activity during carbachol-induced, REM sleep-like atonia. *Am. J. Physiol.*, **275**: R1013-1024, 1998.

Ferini-Strambi L. and Zucconi M. REM sleep behavior disorder. Clin. Neurophysiol., **111** Suppl 2: S136-40, 2000.

Ford B., Holmes CJ., Mainville L., Jones BE. GABAergic neurons in the rat pontomesencephalic tegmentum: codistribution with cholinergic and other tegmental neurons projecting to the posterior lateral hypothalamus. J. Comp. Neurol., **363**: 177-96, 1995.

Fogel SM., Smith CT., Beninger RJ. Increased GABAergic activity in the region of the pedunculopontine and deep mesencephalic reticular nuclei reduces REM sleep and impairs learning in rats. Behav. Neurosci., **124**: 79-86, 2010.

Fortin M. and Parent A. Calretinin-immunoreactive neurons in primate pedunculopontine and laterodorsal tegmental nuclei. *Neuroscience*, **88**: 535-547, 1999.

Fung S.J. and Barnes C.D. Evidence of facilitatory coerulospinal action in lumbar motoneurons of cats. *Brain Res.*, **216**: 299-311, 1981.

Fung S.J., Boxer P.A., Morales F.R., Chase M.H. Hyperpolarizing membrane responses induced in lumbar motoneurons by stimulation of the nucleus reticularis pontis oralis during active sleep. *Brain Res.*, **248**: 267-273, 1982.

Gagnon J.F., Postuma R.B., Mazza S., Doyon J., Montplaisir J. Rapid-eye-movement sleep behaviour disorder and neurodegenerative diseases. *Lancet Neurol.*, **5**: 424-432, 2006.

Garcia-Rill E. The pedunculopontine tegmental nucleus. *Progr. Neurobiol.*, **36**: 363-389, 1991.

Glenn L.L. and Dement W.C. Membrane potential, synaptic activity, and excitability of hindlimb motoneurons during wakefulness and sleep. *J. Neurophysiol.*, **46**: 839-854, 1981a.

Glenn L.L. and Dement W.C. Membrane resistance and rheobase of hindlimb motoneurons during wakefulness and sleep. *J. Neurophysiol.*, **46**: 1076-1088, 1981b.

Habaguchi T., Takakusaki K., Saitoh K., Sugimoto J., Sakamoto T. Medullary reticulospinal tract

mediating the generalized motor inhibition in cats: II. Functional organization within the medullary reticular formation with respect to postsynaptic inhibition of forelimb and hindlimb motoneurons. *Neuroscience*, **113:** 65-77, 2002.

Hendry S.H.C., Jones E.G., Graham J. Thalamic relay nuclei for cerebellar and certain related fiber systems in the cat. *J. Comp. Neurol.*, **185**: 679-714, 1979.

Hikosaka O. and Wurz R.H. Modification of saccadic eye movements by GABA-related substances. II. Effects of muscimol in monkey substantia nigra pars reticulata. *J. Neurophysiol.*, **53**: 292-308, 1985.

Hikosaka O., Takikawa Y., Kawgoe R. Role of the basal ganglia in the control of purposive saccadic eye movements. *Physiol. Rev.*, **80**: 954-978, 2000.

Hirsch E.C., Graybiel A.M., Duyckaerts C., Javoy-Agid F. Neuronal loss in the pedunculopontine tegmental nucleus in Parkinson disease and in progressive supranuclear palsy. *Proc. Natl. Acad. Sci. USA*, **84**: 5976-5980, 1987.

Iranzo A., Molinuevo J.L., Santamaría J., Serradell M., Martí M.J., Valldeoriola F., Tolosa E. Rapid-eye movement sleep behaviour disorder as an early marker for a neurodegenerative disorder: a descriptive study. *Lancet Neurol.*, **5**: 572-577, 2006.

Inglis W.L. and Winn P. The pedunculopontine tegmental nucleus: where the striatum meets the reticular formation. *Progr. Neurobiol.*, **47**: 1-29, 1995.

Jackson A. and Crossman A.R. Nucleus tegmenti pedunculopontinus: efferent connections with special reference to the basal ganglia, studied in the rat by anterograde and retrograde transport of horseradish peroxidase. *Neuroscience*, **10**: 725-765, 1983.

Jones B.E. Paradoxical sleep and its chemical/structural substrates in the brain. *Neuroscience*, **40**: 637-656, 1991.

Jubault T., Brambati S.M., Degroot C., Kullmann B., Strafella A.P., Lafontaine A.L., Chouinard S., Monchi O. Regional brain stem atrophy in idiopathic Parkinson's disease detected by anatomical MRI. *PLoS One*, **4**: e8247, 2009.

Kobayashi Y., Inoue Y., Isa T. Pedunculo-pontine control of visually guided saccades. *Progr. Brain Res.*, **143**: 439-445, 2004.

Kosaka T., Tauchi M., Dahl J. Cholinergic neurons containing GABA-like and/or glutamic acid decarboxylase-like immunoreactivities in various brain regions of the rat. *Expl. Brain Res.*, **70**: 605-617, 1998.

Koyama Y. and Kayama Y. Mutual interactions among cholinergic, noradrenergic and serotonergic neurons studied by iontophoresis of these transmitters in rat brainstem nuclei. *Neuroscience*, **55**: 1117-1126, 1993.

Koyama Y. and Sakai K. Modulation of presumed cholinergic mesopontine tegmental neurons by acetylcholine and monoamines applied iontophoretically in unanesthetized cats. *Neuroscience*, **96**: 723-733, 2000.

Kubin L. Carbachol models of REM sleep: recent developments and new directions. *Arch. Ital. Biol.*, **139**: 147-168, 2001.

Lai Y.Y., Clements J.R., Siegel J.M. Glutamatergic and cholinergic projections to the pontine inhibitory area identified with horseradish peroxidase retrograde transport and immunohistochemistry. *J. Comp. Neurol.*, **336**: 321-330, 1993.

Lai Y.Y., Kodama T., Schenkel E., Siegel J.M. Behavioral response and transmitter release during atonia elicited by medial medullary stimulation. *J. Neurophysiol.,* **104**: 2024-2033, 2010.

Larsen J.P. and Tandberg E. Sleep disorders in patients with Parkinson's disease: epidemiology and management. *CNS Drugs*, **15**: 267-275, 2001.

López-Rodríguez F., Morales F.R., Soja P.J., Chase M.H. Suppression of the PGO-related lumbar motoneuron IPSP by strychnine. *Brain Res.*, **535**: 331-334, 1990.

López-Rodríguez F., Chase M.H., Morales F.R. PGO-related potentials in lumbar motoneurons during active sleep. *J. Neurophysiol.*, **68**: 109-116, 1992.

Luebke J.I., Greene R.W., Semba K., Kamondi A., McCarley R.W., Reiner P.B. Serotonin hyperpolarizes cholinergic low threshold burst neurons in the rat laterodorsal tegmental nucleus in vitro. *Proc. Natl. Acad. Sci. USA*, **89**: 743-747, 1992.

Márquez-Ruiz J. and Escudero M. Eye movements and abducens motoneuron behavior during cholinergically induced REM sleep. *Sleep*, **32**: 471-481, 2009.

Mena-Segovia J., Winn P., Bolam J.P. Cholinergic modulation of midbrain dopaminergic systems. *Brain Res. Rev.*, **58**: 265-271, 2008.

Mena-Segovia J., Micklem B.R., Nair-Roberts R.G., Ungless M.A., Bolam J.P. GABAergic neuron distribution in the pedunculopontine nucleus defines functional subterritories. *J. Comp. Neurol.*, **515**: 397-408, 2009.

Mitani A., Ito K., Hallanger A.E., Wainer B.H., Kataoka K., McCarley R.W. Cholinergic projec-

tions from the laterodorsal and pedunculopontine tegmental nuclei to the pontine giganotocellular tegmental field in the cat. *Brain Res.*, **451**: 397-402, 1988.

Morales F.R., Engelhardt J.K., Soja P.J., Pereda A.E., Chase M.H. Motoneuron properties during motor inhibition produced by microinjection of carbachol into the pontine reticular formation of the decerebrate cat. *J. Neurophysiol.*, **57**: 1118-1129, 1987.

Moriizumi T., Nakamura Y., Tokuno H., Kitao Y., Kudo M. Topographic projections from the basal ganglia to the nucleus tegmenti pedunculopontinus pars compacta of the cat with special reference to pallidal projections. *Exp. Brain Res.*, **71**: 298-306, 1988.

Moruzzi G. and Magoun H.W. Brain stem reticular formation and activation of the EEG. *Clin. Neurophysiol.*, **1**: 455-473, 1949.

Muhlethaler M., Khateb A., Serafin M. Effects of monoamines and opiates on pedunculopontine neurones. In: Mancia M. and Marini G. (Eds.) *The Diencephalon and Sleep*, New York, Raven Press: 31-48, 1990.

Nambu T., Sakurai T., Mizukami K., Hosoya Y., Yanagisawa M., Goto K. Distribution of orexin neurons in the adult rat brain. *Brain Res.*, **827**: 243-260, 1999.

Ottersen O. and Storm-Mathisen J. Glutamate- and GABA containing neurons in the mouse and rat brain, as demonstrated with a new immunohistochemical technique. *J. Comp. Neurol.*, **229**: 374-392, 1984.

Pal D. and Mallick B.N. GABA in pedunculo pontine tegmentum regulates spontaneous rapid eye movement sleep by acting on $GABA_A$ receptors in freely moving rats. *Neurosci. Lett.*, **365**: 200-204, 2009.

Paré D., Curro-Dossi R., Datta S., Steriade M. Brainstem genesis of reserpine-induced ponto-geniculo-occipital waves: an electrophysiological and morphological investigation. *Expl. Brain Res.*, **81**: 533-544, 1990.

Parent A., Mackey A., Smith Y., Boucher R. The output organization of the substantia nigra in primate as revealed by a retrograde double labeling method. *Brain Res. Bull.*, **10**: 529-537, 1983.

Peyron C., Tighe D.K., van den Pol A.N., de Lecea L., Heller H.C., Sutcliffe J.G., Kilduff T.S. Neurons containing hypocretin (orexin) project to multiple neuronal systems. *J. Neurosci.*, **18**: 9996-10015, 1998.

Pierantozzi M., Palmieri M.G., Galati S., Stanzione P., Peppe A., Tropepi D., Brusa L., Pisani A., Moschella V., Marciani M.G., Mazzone P., Stefani A. Pedunculopontine nucleus deep brain stimulation changes spinal cord excitability in Parkinson's disease patients. *J. Neural. Transm.*, **115**: 731-735, 2008.

Pivik R.T., McCarley R.W., Hobson J.A. Eye movement-associated discharge in brain stem neurons during desynchronized sleep. *Brain Res.*, **121**: 59-76, 1977.

Postuma R.B., Gagnon J.F., Rompré S., Montplaisir J.Y. Severity of REM atonia loss in idiopathic REM sleep behavior disorder predicts Parkinson disease. *Neurology*, **74**: 239-244, 2010.

Rinne J.O., Ma S.Y., Lee M.S., Collan Y., Röyttä M. Loss of cholinergic neurons in the pedunculopontine nucleus in Parkinson's disease is related to disability of the patients. *Parkinsonism Relat. Disord.*, **14**:553-557, 2008.

Rye D.B. Contributions of the pedunculopontine region to normal and altered REM sleep. *Sleep*, **20**: 757-788, 1997.

Rye D.B., Saper C.B., Lee H.J., Wainer B.H. Pedunculopontine tegmental nucleus of the rat: cytoarchitecture, cytochemistry, and some extrapyramidal connections of the mesopontine tegmentum. *J. Comp. Neurol.*, **259**: 483-528, 1987.

Rye D.B., Johnston L.H., Watts R.L., Bliwise D.L. Juvenile Parkinson's disease with REM sleep behavior disorder, sleepiness, and daytime REM onset. *Neurology*, **53**: 1868-1870, 1999.

Saitoh K., Hattori S., Song W.-J., Isa T., Takakusaki K. Nigral GABAergic inhibition upon cholinergic neurons in the rat pedunculopontine tegmental nucleus. *Eur. J. Neurosci.*, **18**: 879-886, 2003.

Saitoh K., Isa T., Takakusaki K. Nigral GABAergic inhibition upon mesencephalic dopaminergic cell groups in rats. *Eur. J. Neurosci.*, **19**: 2399-2409, 2004.

Sakai K. and Koyama Y. Are there cholinergic and non-cholinergic paradoxical sleep-on neurones in the pons? *Neuroreport*, **7**: 2449-2453, 1996.

Sakai M., Matsunaga M., Kubota A., Yamanishi Y., Nishizawa Y. Reduction in excessive muscle tone by selective depletion of serotonin in intercollicularly decerebrated rats. *Brain Res.*, **860**: 104-111, 2000.

Saper C.B. and Loewy A.D. Projections of the pedunculopontine tegmental nucleus in the rat: evidence for additional extrapyramidal circuitry. *Brain Res.*, **252**: 367-372, 1982.

Schenck C.H., Bundlie S.R., Mahowald M.W. Delayed emergence of a parkinsonian disorder

in 38% of 29 older men initially diagnosed with idiopathic rapid eye movement sleep behaviour disorder. *Neurology*, **46**: 388-393, 1996.

Semba K. and Fibiger H.C. Afferent connections of the laterodorsal and the pedunculopontine tegmental nuclei in the rat: a retro- and anterograde transport and immunohistochemical study. *J. Comp. Neurol.*, **323**: 387-410, 1992.

Snider R.S. and Niemer W.T. *A stereotaxic atlas of the cat brain.* Chicago: University of Chicago Press, 1961

Soja P.J., Morales F.R., Baranyi A., Chase M.H. Effect of inhibitory amino acid antagonists on IPSPs induced in lumbar motoneurons upon stimulation of the nucleus reticularis gigantocellularis during active sleep. *Brain Res.,* **535**: 331-334, 1987.

Spann B.M. and Grofova I. Nigro-pedunculopontine projection in the rat: an anterograde tracing study with *Phaseolus Vulgaris-Leucoagglutinin* (PHA-L). *J. Comp. Neurol.*, **311**: 375-388, 1991.

Spann B.M. and Grofova I. Cholinergic and non-cholinergic neurons in the rat pedunculopontine tegmental nucleus. *Anat. Embryol.*, **186**: 215-227, 1992.

Stefani A., Lozano A.M., Peppe A., Stanzione P., Galati S., Tropepi D., Pierantozzi M., Brusa L., Scarnati E., Mazzone P. Bilateral deep brain stimulation of the pedunculopontine and subthalamic nuclei in severe Parkinson's disease. *Brain*, **130**:1596-1607, 2007.

Steriade M. Arousal: revisiting the reticular activating system. *Science*, **272**: 225-226, 1996.

Takakusaki K., Ohta Y., Mori S., Single medullary reticulospinal neurons exert postsynaptic inhibitory effects via inhibitory interneurons upon alpha-motoneurons innervating cat hindlimb muscles. *Exp. Brain Res.*, **74**: 11-23, 1989.

Takakusaki K., Kohyama J., Matsuyama K., Mori S. Synaptic mechanisms acting on lumbar motoneurons during postural augmentation induced by serotonin injection into the rostral pontine reticular formation in decerebrate cats. *Exp. Brain Res.*, **93**: 471-482, 1993a

Takakusaki K., Matsuyama K., Kobayashi Y., Kohyama J., Mori S. Pontine microinjection of carbachol and critical zone for inducing postural atonia in reflexively standing decerebrate cats. *Neurosci. Lett.*, **153**: 185-188, 1993b.

Takakusaki K., Shimoda N., Matsuyama K., Mori S. Discharge properties of medullary reticulospinal neurons during postural changes induced by intrapontine injections of carbachol, atropine and serotonin, and their functional linkages to hindlimb motoneurons in cats. *Exp. Brain Res.*, **99**: 361-374, 1994.

Takakusaki K., Shiroyama T., Yamamoto T., Kitai ST. Cholinergic and non-cholinergic tegmental pedunculopontine projection neurons in rats revealed by intracellular labeling. *J. Comp. Neurol.*, **371**: 345-361, 1996.

Takakusaki K. and Kitai S,T. Ionic mechanisms involved in the spontaneous firing of tegmental pedunculopontine nucleus neurons of the rat. *Neuroscience*, **78**: 771-794, 1997a.

Takakusaki K., Shiroyama T., Kitai S.T. Two types of cholinergic neurons in the rat tegmental pedunculopontine nucleus: electrophysiological and morphological characterization. *Neuroscience*, **79**: 1089-1109, 1997b.

Takakusaki K., Kohyama J., Matsuyama K., Mori S. Medullary reticulospinal tract mediating the generalized motor inhibition in cats: parallel inhibitory mechanisms acting on motoneurons and on interneuronal transmission in reflex pathways. *Neuroscience*, **103**: 511-527, 2001.

Takakusaki K., Habaguchi T., Ohtinata-Sugimoto J., Saitoh K., Sakamoto T. Basal ganglia efferents to the brainstem centers controlling postural muscle tone and locomotion; A new concept for understanding motor disorders in basal ganglia dysfunction. *Neuroscience*, **119**: 293-308, 2003a.

Takakusaki K., Kohyama J., Matsuyama K. Medullary reticulospinal tract mediating a generalized motor inhibition in cats: III. Functional organization of spinal interneurons in the lower lumbar segments. *Neuroscience*, **121**: 731-746, 2003b.

Takakusaki K., Habaguchi T., Saitoh K., Kohyama J. Changes in the excitability of hindlimb motoneurons during muscular atonia induced by stimulating the pedunculopontine tegmental nucleus in cats. *Neuroscience*, **124**: 467-480, 2004a.

Takakusaki K., Saitoh K., Harada H., Okumura T., Sakamoto T. Evidence for a role of basal ganglia in the regulation of rapid eye movement sleep by electrical and chemical stimulation for the pedunculopontine tegmental nucleus and the substantia nigra pars reticulata in decerebrate cats. *Neuroscience*, **124**: 207-220, 2004b.

Takakusaki K., Saitoh K., Harada H., Kashiwayanagi M. Role of basal ganglia - brainstem pathways in the control of motor behaviors. *Neurosci. Res.*, **50**: 137-151, 2004c.

Takakusaki K., Takahashi K., Saitoh K., Harada H., Okumura T., Kayama Y., Koyama Y. Orexinergic

projections to the cat midbrain mediate alternation of emotional behavioural states from locomotion to cataplexy. *J. Physiol.*, **568**: 1003-1020, 2005.

Takakusaki K., Saitoh K., Nonaka S., Okumura T., Miyokawa N. Koyama Y. Neurobiological basis of state-dependent control of motor behavior. *Sleep Biol. Rhyth.*, **4**: 87-104, 2006.

Takakusaki K. Forebrain control of locomotor behaviors. *Brain Res. Rev.*, **57**: 192-198, 2008.

Torterolo P., Yamuy J., Sampogna S., Morales F.R., Chase M.H. GABAergic neurons of the laterodorsal and pedunculopontine tegmental nuclei of the cat express c-fos during carbachol-induced active sleep. *Brain Res.*, **892**: 309-319, 2001.

Ulloor J., Mavanji V., Saha S., Siwek D.F., Datta S. Spontaneous REM sleep is modulated by the activation of the pedunculopontine tegmental $GABA_B$ receptors in the freely moving rat. *J. Neurophysiol.*, **91**: 1822-1831, 2004.

Unger M.M., Belke M., Menzler K., Heverhagen J.T., Keil B., Stiasny-Kolster K., Rosenow F., Diederich N.J., Mayer G., Möller J.C., Oertel WH., Knake S. Diffusion tensor imaging in idiopathic REM sleep behavior disorder reveals microstructural changes in the brainstem, substantia nigra, olfactory region, and other brain regions. *Sleep*, **33**: 767-773, 2010.

Vanni-Mercier G., Sakai K., Lin J.S., Jouvet M. Mapping of cholinoceptive brainstem structures responsible for the generation of paradoxical sleep in the cat. *Arch. Ital. Biol.*, **127**: 133-164, 1989.

Vanni-Mercier G. and Debilly G. A key role for the caudoventral pontine tegmentum in the simultaneous generation of eye saccades in bursts and associated ponto-geniculo-occipital waves during paradoxical sleep in the cat. *Neuroscience*, **86**: 571-585, 1998.

Vetrivelan R., Qiu M.H., Chang C., Lu J. Role of basal ganglia in sleep-wake regulation: neural circuitry and clinical significance. *Front. Neuroanat.*, **4**:145, 2010.

Vincent S.R., Satoh K., Armstrong D.M., Fibiger H.C. Substance P in the ascending cholinergic reticular system. *Nature*, **306**: 688-691, 1983.

Vincent S.R. The ascending reticular activating system - from aminergic neurons to nitric oxide. *J. Chem. Neuroanat.*, **18**: 23-30, 2000.

Vitek JL. Deep brain stimulation for Parkinson's disease. A critical re-evaluation of STN versus GPi DBS. *Stereotact. Funct. Neurosurg.*, **78**: 119-131, 2002.

Wichmann T. and Delong M.R. Functional and pathological models of the basal ganglia. *Curr. Opin. Neurobiol.*, **6**: 751-758, 1996.

Williams J.A. and Reiner P.B. Noradrenaline hyperpolarizes identified rat mesopontine cholinergic neurons in vitro. *J. Neurosci.*, **13**: 3878-3883, 1993.

Xi M.C., Morales F.R., Chase M.H. Evidence that wakefulness and REM sleep are controlled by a GABAergic pontine mechanism. *J. Neurophysiol.*, **82**: 2015-2019, 1999.

Xi M.C., Morales F.R., Chase M.H. The motor inhibitory system operating during active sleep is tonically suppressed by GABAergic mechanisms during other states. *J. Neurophysiol.*, **86**: 1908-1915, 2001a.

Xi M.C., Morales F.R., Chase M.H. Induction of wakefulness and inhibition of active (REM) sleep by GABAergic processes in the nucleus pontis oralis. *Arch. Ital. Biol.*, **139**: 125-145, 2001b.

Yamamoto K., Mamelak A.N., Quattrochi J.J., Hobson A.H. A cholinoceptive desynchronized sleep induction zone in the anterodorsal pontine tegmentum: locus of sensitive region. *Neuroscience*, **39**: 270-293, 1990.